Ecological Monographs, 85(1), 2015, pp. 49–72

Fire evolution in the radioactive forests of Ukraine and Belarus: future risks for the population and the environment

N. Evangeliou,[1,13] Y. Balkanski,[1] A. Cozic,[1] W. M. Hao,[2] F. Mouillot,[3] K. Thonicke,[4] R. Paugam,[5] S. Zibtsev,[6] T. A. Mousseau,[7] R. Wang,[1,8] B. Poulter,[1] A. Petkov,[2] C. Yue,[1] P. Cadule,[1] B. Koffi,[9] J. W. Kaiser,[5,10,11] and A. P. Møller[12]

[1]*CEA-UVSQ-CNRS UMR 8212, Institut Pierre et Simon Laplace, Laboratoire des Sciences du Climat et de l'Environnement (LSCE), L'Orme des Merisiers, F-91191 Gif sur Yvette Cedex, France*
[2]*Missoula Fire Sciences Laboratory, Rocky Mountain Research Station Forest Service, Missoula, Montana 59808-9361 USA*
[3]*CEFE UMR 5175, CNRS, Université de Montpellier, Université Paul-Valéry Montpellier, EPHE-IRD, 1919 route de Mende, 34293 Montpellier Cedex 5, France*
[4]*Potsdam Institute for Climate Impact Research (PIK), P.O. Box 60 12 03, 14412 Potsdam, Germany*
[5]*King's College London, London, United Kingdom*
[6]*National University of Life and Environmental Sciences of Ukraine, Kiev, Ukraine*
[7]*Department of Biological Sciences, University of South Carolina, Columbia, South Carolina 29208 USA*
[8]*Laboratory for Earth Surface Processes, College of Urban and Environmental Sciences, Peking University, Beijing 100871 China*
[9]*European Commission, Joint Research Centre, Air and Climate Unit, Ispra, Italy*
[10]*European Centre for Medium-range Weather Forecasts, Reading, United Kingdom*
[11]*Max-Planck-Institute für Chemie, Mainz, Germany*
[12]*Laboratoire d'Ecologie, Systématique et Evolution, CNRS UMR 8079, Université Paris-Sud, Bâtiment 362, F-91405 Orsay Cedex, France*

Abstract. In this paper, we analyze the current and future status of forests in Ukraine and Belarus that were contaminated after the nuclear disaster in 1986. Using several models, together with remote-sensing data and observations, we studied how climate change in these forests may affect fire regimes. We investigated the possibility of ^{137}Cs displacement over Europe by studying previous fire events, and examined three fire scenarios that depended on different emission altitudes of ^{137}Cs, assuming that 10% of the forests were affected by fires. Field measurements and modeling simulations confirmed that numerous radioactive contaminants are still present at these sites in extremely large quantities.

Forests in Eastern Europe are characterized by large, highly fire-prone patches that are conducive to the development of extreme crown fires. Since 1986, there has been a positive correlation between extreme fire events and drought in the two contaminated regions. Litter carbon storage in the area has doubled since 1986 due to increased tree mortality and decreased decomposition rates; dead trees and accumulating litter in turn can provide fuel for wildfires that pose a high risk of redistributing radioactivity in future years. Intense fires in 2002, 2008, and 2010 resulted in the displacement of ^{137}Cs to the south; the cumulative amount of ^{137}Cs re-deposited over Europe was equivalent to 8% of that deposited following the initial Chernobyl disaster. However, a large amount of ^{137}Cs still remains in these forests, which could be remobilized along with a large number of other dangerous, long-lived, refractory radionuclides. We predict that an expanding flammable area associated with climate change will lead to a high risk of radioactive contamination with characteristic fire peaks in the future. Current fire-fighting infrastructure in the region is inadequate due to understaffing and lack of funding. Our data yield the first cogent predictions for future fire incidents and provide scientific insights that could inform and spur evidence-based policy decisions concerning highly contaminated regions around the world, such as those of Chernobyl.

Key words: carbon stock; Cesium-137; Chernobyl; climate change; fire risk; litter; redistribution; wildfires.

Introduction

The April 1986 disaster at the Chernobyl Nuclear Power Plant (ChNPP) in Ukraine (former Soviet Union) resulted from a flawed Soviet reactor design and serious mistakes made by the operators. The ChNPP complex, consisting of four nuclear reactors, is located about 100 km north of Kiev, Ukraine, and about 20 km south of the border with Belarus. Soviet officials began evacuat-

Manuscript received 26 June 2014; revised 29 August 2014; accepted 5 September 2014. Corresponding Editor: A. T. Classen.
[13] Present address: NILU (Norsk institutt for luftforskning), Instituttveien 18, 2007 Kjeller, Norway.
E-mail: Nikolaos.Evangeliou@nilu.no

ing residents near the ChNPP 36 hours after the explosion and by 1990, more than 350 000 people had been displaced and resettled from the most severely contaminated areas of Belarus, Russia, and Ukraine (UNDP and UNICEF 2002). This left a 2600-km^2 area, now known as the Chernobyl Exclusion Zone (CEZ), empty of humans. However, around 600 000 emergency workers were drafted to clean up the contamination and manage the remaining three reactors (the last of which closed in December 2000) and large amounts of contaminants still remain inside. North of the border with Ukraine, Belarusian authorities created a similar 2200-km^2 restricted zone.

Thousands of hectares of a largely rural area were severely contaminated as a result of the accident. Forests and fields were subjected to a dense cloud of radioactive fallout that included ^{137}Cs (half-life 30.2 years), ^{90}Sr (half-life 28.8 years), multiple isotopes of plutonium, and other radionuclides (NEA 2002). Among the tasks of the cleanup workers (known as "liquidators") were felling, bulldozing, and burying all the trees in a 4 km radius around the ChNPP. They also constructed a series of dikes designed to prevent flooding into the Pripyat River, and from there into the Dnieper River, which flows through Kiev to the Black Sea. Most of the contamination sank into benthic river and reservoir sediments, where it is supposedly stable (IAEA 2006).

With no one to cut saplings and cultivate fields, natural ecological succession has gradually transformed the landscape. Forests that covered 53% of the area before the disaster now cover more than 70% (IAEA 2001). Stands dominated by birches (*Betula pendula*) and pines (*Pinus sylvestris*) have taken over pastures where farmers formerly grew wheat and flax. Most pines (which are more sensitive to radiation than birches; Yoschenko et al. 2011) seem normal, although deformed trees are common in contaminated areas and substantial negative effects of radiation on tree growth have been reported (e.g., Mousseau et al. 2013).

Radionuclides have migrated into the forest soil and, for the most part, remain there. Studies have shown that 90% of ^{90}Sr is located in the top 10 cm of the soil (IRL 2013), whereas Yablokov et al. (2009) reported that 80% of ^{137}Cs remained in the top 5 cm in the area. As trees, grasses, other plants, and fungi transpire (release water), they draw water up from the roots. Water-soluble salts of cesium and strontium are chemical analogues of potassium and calcium, respectively, and are taken up in place of these crucial nutrients. The leaves fall to the ground in autumn, becoming part of the "litter" (the abscised vegetation that covers the forest floor), thus returning the radioactive salts to the top layer of the soil. Without the presence of trees or other permanent groundcover, contaminants would likely migrate out of the soil by being dispersed in dust or carried by water.

People living just outside the exclusion zone, who depend on forests for work, food, fuel, and other resources, pay the cost for this environmental contamination. Many continue to live in areas with ^{137}Cs soil concentrations greater than 37 kBq/m^2. They also continue to eat mushrooms, berries, and other local forest foods, despite government restrictions and warnings (NEA 2002). Mushrooms, which are highly prized by local populations, absorb high concentrations of radioactive cesium (Linkov et al. 2000). Although ^{137}Cs content in the majority of edible mushrooms decreased by 20–30% between 2005 and 2010, fungal species whose feeding networks (mycelia) reach deeper into the soil showed substantial increases in the amount of ^{137}Cs during the same period as radionuclides migrated into deeper soil layers (NRU 2011).

Chernobyl contamination is also affecting non-human communities. Although it has been reported that the absence of people has attracted a surprising amount of wildlife, scientific surveys suggest that the populations of many mammals and birds are not as diverse or abundant as would have been expected in a region where there is little pressure from human communities (Møller and Mousseau 2013). Fewer mammals live and reproduce in high-radiation areas than in less contaminated ones (Møller and Mousseau 2013). Birds show reduced longevity and male fertility, smaller brains, and increased frequency of mutations that indicate significant genetic damage (Møller et al. 2012). Likewise, some bird populations in contaminated areas are only sustained via immigration from adjacent uncontaminated regions (Møller et al. 2006).

Ukrainian law requires that the exclusion zone should be managed as a barrier that fixes contamination through natural processes; everything deposited in 1986 must stay within the guarded area. Prohibiting residence and economic activities such as commercial forestry helps keep contaminated materials inside the zone. The effectiveness of such laws is often challenged, however, since many trucks transporting large logs of pine and other trees have been observed in CEZ during the summer of 2013 (A. P. Møller, *personal observations*).

Proponents of extensive decontamination in Chernobyl see many benefits beyond public safety including (1) more productive timber plantations (thousands of hectares were in need of thinning even before the disaster); (2) jobs; and (3) a sustainable energy source (if debris can be burned in biomass power plants). On the other hand, uncontrolled burning of contaminated wood may negate these putative benefits by spreading contaminants far beyond their current locations. Trees and other groundcover that are currently trapping radionuclides may become more susceptible to fire. The stands that now grow on approximately 1800 km^2 are largely unmanaged. As trees mature and die and more sunlight penetrates the canopy, brush and other understory species are starting to grow. The Chernobyl forests are thus developing "fuel ladders" of vegetation that would enable a fire to climb into the tree canopy and burgeon into a crown fire (Hao et al. 2009). A lack

of effective forest management, combined with a general drying trend attributable to local climate change, could lead to catastrophic fires more intense than those already seen in Chernobyl.

When forests laden with radionucleotides burn, they emit radioactive cesium, strontium, and plutonium in respirable fine particles (Hao et al. 2009). Here, we use the terms displacement or redistribution of ^{137}Cs to define the amount of ^{137}Cs present in the vegetation, soil, or litter, which would be emitted in the atmospheric aerosol after a major fire. High-intensity crown fires in Chernobyl would release large amounts of radionuclides and transport these emissions hundreds to thousands of kilometers to human population centers (Hao et al. 2009). Such contamination could trigger long-term, economically damaging government restrictions on contaminated milk, meat, and vegetables.

The Ukrainian government faces the challenge of protecting its citizens, even as it strives to return residents to the rural communities that would provide them with clean water, food, firewood, and livelihoods. Whether Ukraine opts for leaving forests to their slow but natural recovery or attempts to decontaminate them, local residents will inevitably be affected by ongoing contamination. These effects may be exacerbated by the current political instability in Ukraine and a reduction in the priority of forest management and changes in fire fighting policy due to other governmental activities. Therefore, the primary aim of present paper is to alert the scientific community about how changes in Chernobyl forests, accompanied by pronounced climatic changes, could remobilize radioactivity. Another aim is to provide scientific insights that could motivate and inform evidenced-based policy decisions concerning radioactively contaminated regions around the world.

In this paper, we explicitly investigate a number of hypotheses to address the two aims listed in the previous paragraph. We do so by focusing on two areas with the highest deposition density after the Chernobyl accident, namely (1) a region centered at the ChNPP between 29° E to 31° E and 50.5° N to 52° N where deposition density ranges from 40 to more than 1480 kBq/m^2 and (2) a highly contaminated zone 50 km northeast of the NPP in Belarus (30.5° E to 32.5° E and 52° N to 53.5° N). The International Atomic Energy Agency (IAEA 2005, 2009) defines any area with surface activity larger than 40 kBq/m^2 (for beta and gamma emitters) as contaminated. In a first hypothesis, we test to what extent wildfires in contaminated regions of Ukraine and Belarus result in atmospheric transport and redeposition of radionuclides. To this end, we analyze the wildfires of 2002, 2008, and 2010 in the contaminated regions of Ukraine and Belarus and document the atmospheric transport and "new" deposition of ^{137}Cs throughout Europe after its redistribution by fires. Cesium-137 is among the most dangerous radionuclides released after nuclear accidents, due to its long half-life, the radiation type it emits during decay, and its bioaccumulation by organisms (Woodhead 1973). The second hypothesis posits that atmospheric transport of ^{137}Cs in smoke will depend on injection heights. The effect of the injection height of ^{137}Cs (present in smoke) on atmospheric transport is determined by investigating three fire scenarios that differ only by their injection heights. The third hypothesis suggests that the frequency and magnitude of fires will depend on the development of the vegetation and climate change. To this end, we model the occurrence of future fires (2010–2100) in the area, incorporating several different models (e.g., for vegetation and fire) and satellite data (e.g., MODIS) in order to reduce uncertainty and to present realistic past, present and future predictions of the hazards and risks from radioactivity redistribution by wildfires. Based on our findings, we recommend policy changes aimed at preventing further future contamination. To our knowledge, this is the first paper in which the effects of climate change on wildfires are studied in relation to radionuclide mobility.

Databases and Methodology

Databases for climate model diagnosis and inter-comparison

Temperature and precipitation fields in contaminated areas of Chernobyl were taken from the Program for Climate Model Diagnosis and Inter-comparison (PCMDI) databases. PCMDI was established in 1989 at the Lawrence Livermore National Laboratory (USA) and aims to develop tools for the diagnosis and inter-comparison of general circulation models (GCMs) that simulate global climate. The GCMs adopted here are from the modeling groups of the Canadian Centre for Climate Modeling and Analysis (CCCMA); the CSIRO atmospheric research (CSIRO); the U.S. Department of Commerce, NOAA, Geophysical Fluid Dynamics Laboratory (GFDL); the NASA Goddard Institute for Space Studies (GISS); the Institut Pierre et Simon Laplace (IPSL); the Meteorological Institute of the University of Bonn (MIUB); the Max Planck Institute for Meteorology (MPI); the National Center for Atmospheric Research (NCAR); and the Hadley Center for Climate Prediction and Research, Met Office (UKMO).

Global Fire Emissions Database (GFED3) and Standardized Precipitation–Evapotranspiration Index (SPEI) database

Satellite data on fire activity and vegetation productivity were combined to estimate gridded burned area and fire emissions. The GFED3 database (which combines multiple satellite fire products for better accuracy and longer time series [Giglio et al. 2010]), was used to estimate burned area, because it constitutes the current reference data set available for all over the world (Mouillot et al. 2014; GFED3 database *available online*).[14] The database offers burned area for each 0.5° resolution pixel globally, on a monthly time step, and the subsequent emissions due to biomass burning,

[14] http://www.falw.vu/~gwerf/GFED/GFED3/emissions/

including carbon (CO, CO_2), methane and non-methane hydrocarbons, NO_x, SO_2, and particulate matter. Emissions were based on a global estimation of fuel biomass and moisture content simulated by the biogeochemical model CASA (Potter et al. 1993), coupled with a combustion module (Van der Werf et al. 2003), using emissions factors from Akagi et al. (2011).

As fire-spread is the result of a combination between fuel moisture, fuel amount, and landscape pattern (Cary et al. 2006, Krawchuk and Moritz 2011), we investigated the continental-scale fire regime as a response to drought, tree cover, and forest patch presence. Drought effects are apparent only after a long period with a shortage of precipitation, making it very difficult to objectively quantify the characteristics of drought episodes in terms of their intensity, magnitude, duration, and spatial extent. We selected SPEI as an integrative drought index, which calculates normalized monthly drought anomalies as the precipitation/potential evapotranspiration differences compared to the average calculated over the whole time series. SPEI is expressed according to the time frame and the month considered for calculation and is available at a 0.5° resolution globally for the period 1901 to the present (Vicente-Serrano et al. 2012); for instance, we selected the SPEI03 for September corresponding to the integrated drought index over the three months before September (summer). Statistical analysis for the temporal trend in the SPEI03 was performed using the non-parametric Mann-Kendall trend test using the Kendall R package and the Tukey honestly significant difference (tukeyHSD function using R [R Development Core Team 2014]) for comparing burned area distribution among SPEI03 drought classes.

Continental-scale fuel biomass and landscape structure were investigated from tree cover. Kempeneers et al. (2011) provided data of different remote-sensing products to produce an accurate tree cover map at 1-km resolution for Europe, including Ukraine and Belarus (Appendix: Fig. A1) as a surrogate for the Corine Land cover, from which Eastern Europe is not included. Landscape indices of largest patch index (LPI) and mean patch area (MPA) were calculated (Fragstats; MacGarigal and Marks 1994) for each 0.5° cell over Europe based on forest patch analysis derived from the tree cover map reclassified into forest/non forest at a 50% tree cover threshold.

Moderate Resolution Imaging Spectroradiometer (MODIS) area burned data

To document the multiple fires that occurred in the two areas of interest, we used the MODIS direct broadcast (DB) algorithm developed by Urbanski et al. (2009), which combines active fire detection and burn scar detections in single satellite scenes to map burned areas with a nominal spatial and temporal resolution of 500 m and 1 day, respectively. The MODIS-DB algorithm provides rapid mapping of burned areas and enables production of a regional emission inventory within 1 hour of the final (Aqua satellite), local MODIS overpass. Although the algorithm was designed to process DB data in near-real time, archived data were used (Urbanski et al. 2011) to monitor the spatial and temporal distribution of fires, smoke, vegetation, and flooding in the two contaminated areas. The dates and the spatial distribution of fires were determined from MODIS active fires for the years 2002, 2008, and 2010. For the three fire scenarios that assumed that 10% of the contaminated area is burned (2010 scenario 6, 2010 scenario 7, and 2010 scenario 8), we kept the same temporal pattern with the fires of 2010 in the area. MODIS area burned (250 000 m^2 per pixel) was combined with ^{137}Cs deposition densities (kBq/m^2) and the respective emission factors to estimate ^{137}Cs emission per pixel.

Biomass burning estimates using PKU-FUEL

Inventories of firewood and straw consumption in the domestic sector, as well as agricultural solid waste burning in the fields, were derived from PKU-FUEL (Peking University Fuel Inventory) for the year 2007 at $0.1° \times 0.1°$ resolution (Wang et al. 2013); the product covers 36 European countries for the year 2007. The same inventories for 1986 ($0.1° \times 0.1°$) data were derived by scaling the gridded data with the ratio of national consumptions between 1986 and 2007. Specifically, the national consumption of firewood and agricultural solid waste burning were collected from FAO (2013), and the data on domestic straw consumption from IEA (2013). The projections show the temporal change of firewood and straw consumption in the area, as well as changes in agricultural burning since the date of the accident.

Assumptions on the redistribution of ^{137}Cs

Only four references were found in the relevant literature and taken into consideration in order to define the amount of ^{137}Cs emitted after fires (hereafter, emission factor). Yoschenko et al. (2006) used three natural experimental sites in the CEZ. They measured background radiation, soil, natural litter, and vegetation and then estimated the budget, concluding that the redistribution of ^{137}Cs after fires was at least 4%. Amiro et al. (1996) carried out experimental burning of straw, pine, and Norway maple (*Acer platanoides*) recording several physicochemical characteristics such as temperature and moisture of the fuel. They concluded that the redistribution of ^{137}Cs is a highly variable process depending on the fire temperature and the type of vegetation in the fuel and may range from 20% to 100%. Horrill et al. (1995) performed experimental burns of heather (*Calluna vulgaris*) in an area of Scotland that was intensely affected by the Chernobyl accident, since heather has been found to accumulate higher levels of radiocesium than many other upland plants (Bunzl and Kracke 1984). They found that 10–40% of ^{137}Cs would be lost after a heather fire, strongly depending on the

temperature (12% after cool burning and 39% after hot burning). Piga (2010) performed similar fire experiments in an artificial experimental site at the Institut de Radioprotection et de Sûreté Nucléaire, France, using contaminated wood as fuel. He recorded ^{137}Cs levels before and after burning, as well as the emitted amount in the ambient aerosol, concluding that the redistribution was approximately 10%. These studies indicate that the redistribution of ^{137}Cs strongly depends on the temperature of the fire and the type of vegetation used as fuel. Most of the aforementioned studies were based on experiments in which controlled conditions were maintained, whereas our study aimed to analyze uncontrolled wildfires. Given that the prevailing temperatures in a wildfire are higher than the controlled experiments, we expected the redistribution of ^{137}Cs to be close to that estimated by Horrill et al. (1995) for hot burning, corresponding to approximately 40%.

We also addressed the fate of ^{137}Cs deposited in the soil and the amount redistributed after fires. Analyses of data collected after Chernobyl, and recently after Fukushima (e.g., Hashimoto et al. 2012) have shown that ^{137}Cs is accumulated in the topsoil layer (Filipovic-Vincekovic et al. 1991, Avery 1996) and remains there for many years with a migration velocity of approximately 0.09 cm/yr (Lujanieneo et al. 2002). Once deposited, ^{137}Cs is affected by many site-specific factors including soil type, rainfall, drainage, terrain, vegetation, and local activities and conditions. Studying four different contaminated sites in Chernobyl in 1991, Poiarkov (1995) showed that 84–86% of ^{137}Cs predominated in the litter and the first 2 cm of the soil, whereas the remainder migrated into deeper layers of the soil. The fraction of ^{137}Cs in topsoil was much higher in Fukushima (97%) one year after the accident (Tanaka et al. 2012). The cesium cation (the predominant species of Cs in aqueous solution) interacts strongly with many soils due to its low tendency to hydrate and higher polarizability than smaller ions like K^+ (Avery 1996). Its binding in soils is largely contingent on the content of inorganic minerals relative to organic matter. The organic fraction of soils has a larger cation exchange capacity than inorganic soil particles. Organic matter can bind Cs^+, acting as a transfer parameter for Cs (De Brouwer et al. 1994, Shand et al. 1994, Lujanieneo et al. 2002). Since ^{137}Cs has a relatively low boiling point of 669°C, it is partially volatilized in smoke even when bound in soil. Paliouris et al. (1995) showed that more than 20% of ^{137}Cs is redistributed by large fires in North American boreal forests. Due to the lack of such studies in highly contaminated areas, and for simplicity's sake, we assumed that this ratio was the same as that for the redistribution of ^{137}Cs following burning (40%).

The transport model

The coupled model LMDZORINCA was used in the simulations (Szopa et al. 2012) consisting of the aerosol module INCA (INteractions between Chemistry and Aerosols), the general circulation model (GCM), LMDz, (Laboratoire de Météorologie Dynamique), and the global vegetation model ORCHIDEE (ORganizing Carbon and Hydrology In Dynamic Ecosystems Environment). The model accounts for emission, transport, photochemical transformations, and dry and wet scavenging of chemical species and aerosols (Evangeliou et al. 2013). The horizontal resolution of the model in the regular grid is 1.27° in latitude and 2.50° in longitude, whereas the vertical grid is divided into 19 levels from the surface up to about 3.8 hPa. However, the GCM also offers the opportunity to stretch the grid over specific regions using the same number of grid-boxes. In the present study, the fire incidents were simulated using the zoom version for Europe, achieving a horizontal resolution of 0.51° × 0.45° for 19 vertical levels. The model can be run in a nudged mode using the ERA40 reanalysis data, with 6-h wind fields, by the European Centre for Medium-Range Weather Forecasts (ECMWF 2002) with a relaxation time of 10 days for the regular grid; in the zoom version, the model was relaxed to 4.8 days in the center of the zoom and to 10 days outside (Hourdin and Issartel 2000).

Wildfires in the years 2002, 2008, and 2010 were simulated, and three extreme fire scenarios were also studied assuming that 10% of the contaminated forests were burned following different injection regimes described in detail in *Estimates of the altitude of the emissions near Chernobyl and Belarusian forests using the Plume Rise Model (PRM)* (2010 scenario 6, 2010 scenario 7, and 2010 scenario 8). Each simulation lasted from March to the end of the year. According to relevant measurements of ^{137}Cs activity concentrations after the recent accident of Fukushima, the detection of ^{137}Cs in the ambient aerosol ended 2–3 months after the initial emissions (Masson et al. 2011, Long et al. 2012, McMullin et al. 2012, Paatero et al. 2012); therefore, one year was sufficient to obtain an overall view of the deposition of ^{137}Cs after wildfires.

Estimates of the altitude of the emissions near Chernobyl and Belarusian forests using the Plume Rise Model (PRM)

Current deposition densities were needed in order to estimate the redistribution of ^{137}Cs after fires. Therefore, we used the Radioactivity Environmental Monitoring (REM) database (De Cort et al. 1998), combined with measurement data adapted from Kashparov et al. (2003), assuming an effective half-life of ^{137}Cs of 10 years. Bergan (2000), in the first complete study about ecological loss of ^{137}Cs, reported that "the calculated effective half-lives of radiocesium in the surface soil layer vary across the sites from 10 to 30 years, which is equal to the physical half-life of ^{137}Cs". Effective half-life of ^{137}Cs combines its physical decay and also its ecological half-life (which includes all environmental removing processes, such as vertical migration, runoff to large reservoirs, soil erosion, etc); hence, the data were

corrected for 1 March 2002, 2008, and 2010. The data were validated using measurement-based maps reported in the NRU (2011).

Once aloft, air currents can transport fire emissions, affecting their longevity, chemical conversion, and fate. Models and observations (e.g., Chin et al. 2002, Bertschi et al. 2004) have shown that aerosol residence times in the atmosphere and downwind effects on surface air quality depend on the heights at which emissions are injected. In a study of 1998 boreal fires, Leung et al. (2007) concluded that at least half of the carbon is injected above the boundary layer (3–5 km) as a result of convection. Studies of crown fires have shown that many fires generate sufficient energy to loft smoke plumes above the boundary layer (Cofer et al. 1996, Lavoue et al. 2000) up to stratospheric altitudes by supercell convection (Fromm and Servranckx 2003, Fromm et al. 2008). The goal here was to generate realistic parameterizations for the injection heights of forest fire scenarios to be used in our global atmospheric model.

Chemical transport models (CTMs) are used to quantify these processes. Unlike all other emissions (except for those from aircraft and volcanoes), fires may inject their smoke plumes into the troposphere, and occasionally even into the lower stratosphere, by virtue of the intense radiative energy and convection produced by the burning fuel. The dynamics of the plume responsible for the updraft and its final emission profile take place at scales than range below CTM resolution and therefore cannot be modeled; thus, parameterization is usually needed to predict fire injection height at a large scale. Several plume models have already been implemented in CTMs, each of them focusing on different aspects of plume dynamics. The PRM of Freitas et al. (2007, 2010) emphasizes the role of moist convection and ambient wind shear. Rio et al. (2010) developed a model that, together with modeling water transport within the plume, can interact with ambient stratification. Sofiev et al. (2012) derived an empirical model from dimensional analysis and optimization, using as input the fire radiative power (FRP), to model the convection induced by the fire, and the Brunt-Vasisala frequency above the boundary layer to model the effect of atmospheric stability. To our knowledge, these parameterizations have not been properly validated. However, Val Martin et al. (2013) used the Multi-angle Imaging SpectroRadiometer (MISR) injection height data set to run a fire-by-fire comparison, and concluded that the performance of the PRM was not reliable. Such validations on a fire-by-fire basis are problematic in that the main source of available data, the MISR injection height data set, might be biased by the fact that fire observations occur in most cases early in the morning when fire intensity and plumes are not yet mature.

Recently, a new approach based on the original version of PRM has been developed to introduce additional physical constraints (Paugam et al. 2010). In the new PRM2 model, an equation for mass conservation was added, the fire-induced convection was derived from FRP measurements, and the entrainment and detrainment scheme was improved to adapt to more atmospheric scenarios. Six parameters were introduced and optimized to fit well-characterized fire events. The selection of these particular fires was made through the MISR data set, and fires were detected when effects of the diurnal cycle (high-latitude fires had more Terra overpasses, and so had MISR observations made later in the day), or the time lag between fire radiation and plume development (use of multiple overpass form Terra and Aqua are used to only consider mature fire) could be considered negligible. For each fire a detrainment profile was computed, allowing estimation of the ratio of burned mass emitted in the boundary layer and above it at the scale of every single fire. Fig. 1 shows results of the PRM2 model applied to fires detected by MODIS (for both Terra and Aqua sensors) in the Ukrainian and Belarusian forests for the years 2003, 2008, and 2010. It shows the average and maximum injection height above the boundary layer, the maximum injection height above the ground, the number of fires, and the total fire radiative energy (FRE) in the selected area. Fig. 1 emphasizes the variability of injection height (with injection up to 7 km) and mean injection heights above the boundary layer (top panels) and the dependence on the atmosphere, as the maxima above the boundary layer do not necessarily match with the maximum height above the ground or the fire activity.

For all these reasons, we assumed ^{137}Cs would follow the same dynamics with fire emissions from the PRM2 and therefore, a mean vertical mass profile was computed and applied to the ^{137}Cs emission from fires. Due to the lack of data in 2002, we used the vertical distribution of the plume for 2003 (a more conventional distribution), in which the maximum injection height reached 2.9 km. For 2008 fires, in which larger injection heights were obtained by the PRM2 model (FRE was extremely high, reflecting the high fire intensity), the upper limit of the injection was set to 6 km. For the large fires of 2010, a maximum emission altitude of 4.3 km was chosen on the basis of the results presented in Fig. 1. Val Martin et al. (2010) and Kahn et al. (2008) showed that fires in boreal forests of North America and Alaska resulted in smoke injections above the boundary layer. In addition, Sofiev et al. (2013) published global maps of emission heights and the resulting vertical profiles for wildfires that occurred between 2000 and 2012. They concluded that regions with moderately high injection heights include forests in Amazonia, equatorial and southern Africa, and central Eurasia, where 90% of the mass is emitted within the lowest 3 km of the atmosphere (the boundary layer in these forests can be seen in Appendix: Fig. A2). These regions are notable for quite strong fires and deep boundary layers (van der Werf et al. 2010), and include the Ukrainian and Belarusian forests. The profiles used here were compa-

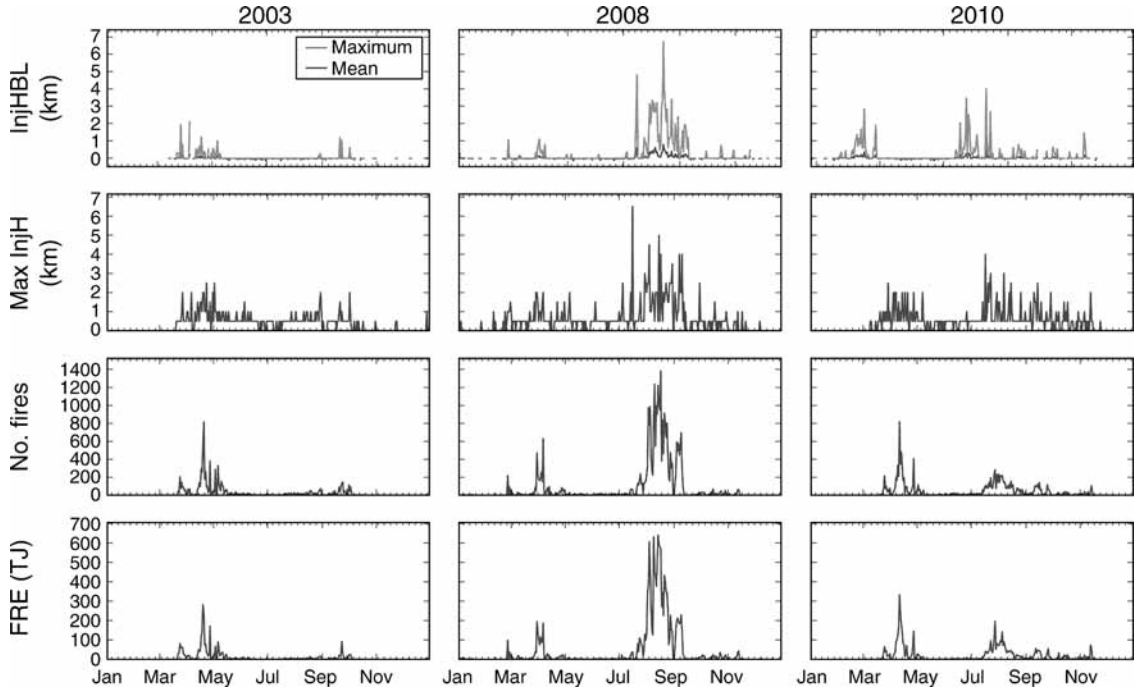

FIG. 1. Mean and maximum injection height above the boundary layer (InjHBL; km), maximum injection height above the ground (max InjH; km), number of fires, and total fire radiative energy (FRE) in the selected area for the fires in 2002, 2008, and 2010.

rable to those presented by Sofiev et al. (2013), wherein ~90% of ^{137}Cs is emitted within 3 km height. Finally, three extreme scenarios were also studied (10% of the contaminated area burns), accounting for a maximum injection at 2.9 km (2010 scenario 6), 4.3 km (2010 scenario 7), and up to 6 km (2010 scenario 8) using the same profiles of the fire years 2002, 2010, and 2008, respectively. The spatial deposition density of ^{137}Cs (Bq/m^2) in these forests is multiplied with the burned area (m^2) from MODIS and the emission factor (40%), in order to estimate ^{137}Cs emissions after fires.

LPJmL-SPITFIRE coupled model for litter carbon storage

A process-based fire regime model, SPread and InTensity of FIRE (SPITFIRE; Thonicke et al. 2001), coupled with ecosystem dynamics in the LPJmL (Lund, Potsdam, and Jena) Dynamic Global Vegetation Model (Sitch et al. 2003, Gerten et al. 2004, Bondeau et al. 2007) was used to explore relationships between litter carbon stock and fire tendency from 1986 to 2010. The aim was to study past, present, and future effects of fires on the terrestrial carbon cycle and the associated emissions of trace atmospheric constituents. The same coupled configuration was used to estimate future burned areas and litter carbon storage in Europe and specifically in contaminated regions of Ukraine and Belarus up to 2100 under the REMO-A1B climate change scenario. Comparison with observed active fire counts have shown that the model reproduces fire occurrence and can mimic broad geographic patterns during the peak fire season. Modeled fire season duration is generally overestimated by about one month, but shows a realistic pattern of differences among biomes. Comparisons with remotely sensed burned area products have indicated that the model reproduces broad geographic patterns of annual fractional burned area over most regions, including the boreal forest (Thonicke et al. 2010).

RESULTS

Climate change in Chernobyl and Belarus

Empirical observations over the past century have shown that temperatures at the surface have risen globally, with important regional variations. Global average warming has been increasing since 1900, with a trend between 0.07° ± 0.02°C per decade to 0.13° ± 0.03°C per decade (Scafetta and West 2006). Observations of global precipitation have shown that variability exists in the amount, intensity, frequency, and type of precipitation. Temperatures in Ukraine and Belarus have become increasingly warmer in spring and summer since 1950, and precipitation has decreased (or remained stable) considerably during the same period (Fig. 2). The most pronounced increase occurred during July–August 2010, when temperatures exceeded 40°C accompanied by many weeks without precipitation. With the projected increase in CO_2 and other greenhouse gases, most coupled models predict an increase in the occurrence

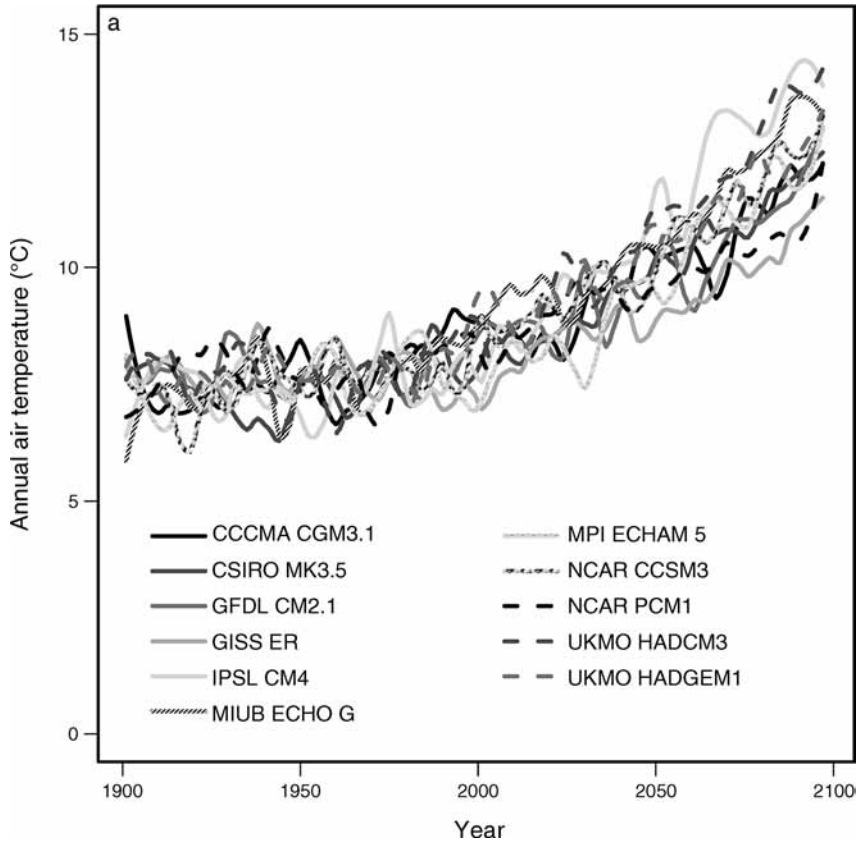
a
Annual air temperature (°C)
15
10
5
0
1900
1950
2000
2050
2100
Year
CCCMA CGM3.1
CSIRO MK3.5
GFDL CM2.1
GISS ER
IPSL CM4
MIUB ECHO G
MPI ECHAM 5
NCAR CCSM3
NCAR PCM1
UKMO HADCM3
UKMO HADGEM1

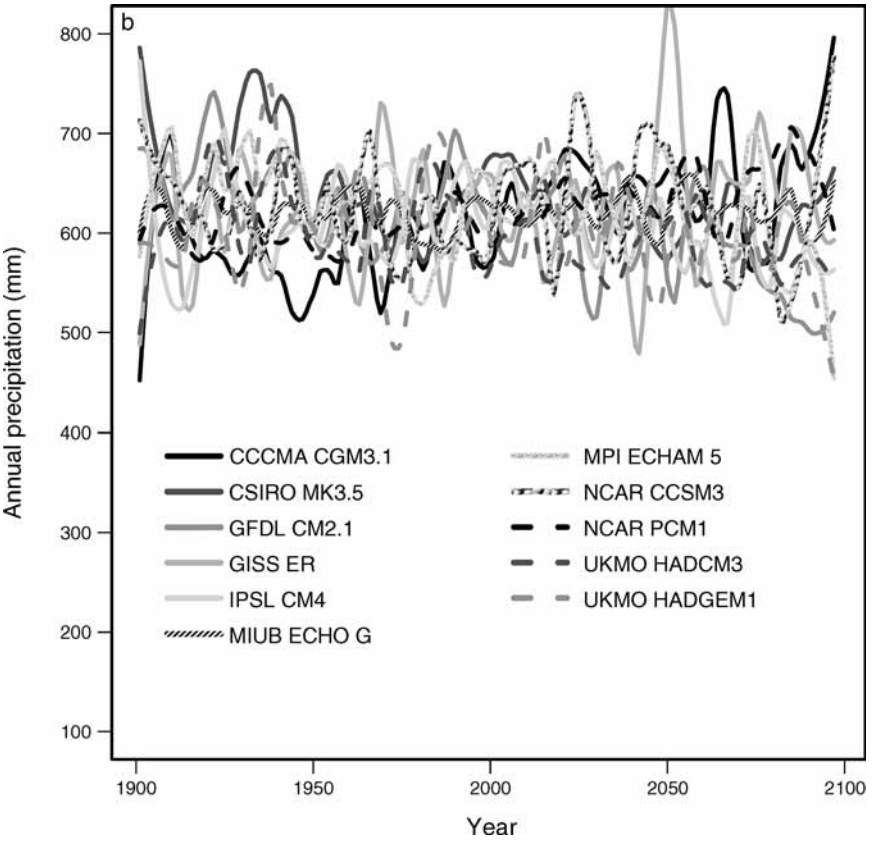
b
Annual precipitation (mm)
800
700
600
500
400
300
200
100
1900
1950
2000
2050
2100
Year
CCCMA CGM3.1
CSIRO MK3.5
GFDL CM2.1
GISS ER
IPSL CM4
MIUB ECHO G
MPI ECHAM 5
NCAR CCSM3
NCAR PCM1
UKMO HADCM3
UKMO HADGEM1

of exceedingly warm and dry summers in the future (Fig. 2).

Recent fire history as seen from GFED3 burned area database

Annual average and maximum values of burned area (BA), total carbon (TC), and total particulate matter (TPM) for Europe derived from the GFED3 database are presented for the 1997–2009 period in Appendix: Fig. A3. The most fire-prone areas were the grasslands of Eastern Europe and the Mediterranean forests with an average of 5000 ha/cell unit (0.5°) corresponding to 2% of the cell. Annual maximum burned area reached 50 000 ha (20% of the grid cell) during extreme fire years. TC and TPM emitted during fire events depended on the fuel amount available for burning; for example, except for acting as a spreading agent, grassland steppes remained a very large atmospheric emitter during fires in the same range with forest ecosystems of high fuel amounts (Appendix: Fig. A2). Located at the interface between grassland steppes and the temperate/boreal biomes, Ukraine is affected by both recurrent grassland fires and less-frequent but more intensively emitting forest fires.

The largest burned areas in Europe during the last decade occurred in 2003 and 2005 (Fig. 3). In 2001, fires were widespread in the Eastern Mediterranean and Ukraine, whereas 2003 was the most extreme year for fires in grassland steppes. Very important forest fires occurred in Portugal, northern Ukraine, and Greece in 2005 and 2007, and fires burned considerable forest areas in Russia in 2008. Burned areas varied between 100 000 ha in 1997 to 837 000 ha in 2003, with an average of 260 000 ha in Europe (JRC 2014).

Fire activity and drought in Europe

According to the "varying constraint hypothesis" (Krawchuk and Moritz 2011), fire activity is a function of the fuel amount available. Increasing drought affects fire activity differently depending on the availability of fuel. The last increases fire risk in fuel-unlimited areas as a consequence of low fuel moisture content, while decreases fire risk in fuel-limited areas by reducing net primary production and in turn fuel accumulation. Using the summer SPEI03 drought index time series for the period 1901–2009 we computed the driest and wettest extreme years for the 1997–2008 period over Chernobyl (Fig. 4a). The driest years (minimum SPEI03) in the regions of interest were 2003 for northwestern Europe (due to the extreme heat wave),

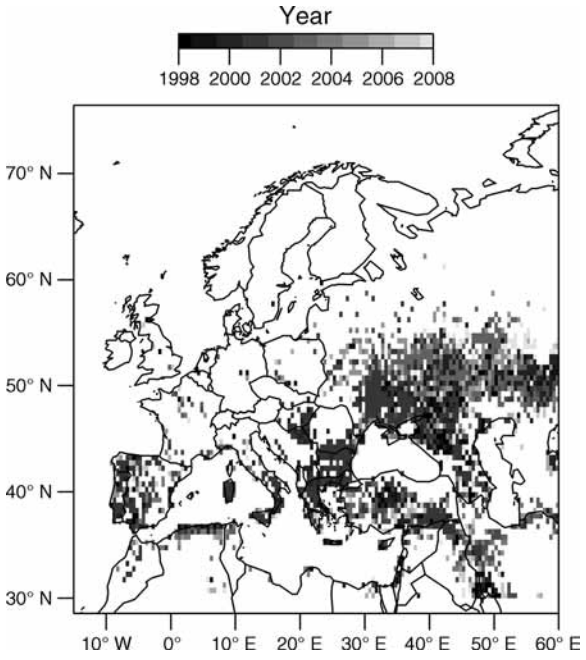

FIG. 3. Continental distribution of maximum fire year in Europe for 1997–2008 based on the GFED3 database.

2005 in Portugal and northern Russia, 2007 for the Eastern Mediterranean, and 2000 and 2001 for the Balkan countries. We identified the wettest year (maximum SPEI03) as 2003 for the grassland steppes in Eastern Europe (Fig. 4b and c). When comparing these maps with the highest fire years from GFED3, the year 2001 did not appear to be extremely dry, although it was an intense fire year. However, the dry years 2005 and 2007 were identified as intense fire years in Portugal and the Eastern Mediterranean, respectively. We particularly focused on high-biomass forested ecosystems potentially leading to high particulate emissions. We cross-tabulated annual anomalies of burned area occurring in forests (by combining GFED3 and the tree cover map) with summer SPEI03 anomalies. We observed that significantly more burned areas occur during drier years (negative SPEI03; Tukey test, $P < 0.05$) compared to average (SPEI03 around 0) or wetter (SPEI03 > 0) years (Fig. 4d). This is a generic pattern observed worldwide (Hessl et al. 2004, Xiao and Zhuang 2007). Since forest fire activity was correlated with summer drought, the temporal trend of summer SPEI03 was tested over the CEZ (Fig. 4a). A significant negative trend (Mann-Kendall Test, $P < 0.1$) was observed for the recent years (significant

←

FIG. 2. Annual land-surface air temperature (°C) and precipitation (mm) between 1900 and 2100 in Chernobyl and Belarus. The GCMs adopted here are from the modeling groups of the Canadian Center for Climate Modeling and Analysis (CCCMA); the CSIRO atmospheric research (CSIRO); the U.S. Department of Commerce, NOAA, Geophysical Fluid Dynamics Laboratory (GFDL); the NASA Goddard Institute for Space Studies (GISS); the Institut Pierre et Simon Laplace (IPSL); the Meteorological Institute of the University of Bonn (MIUB); the Max Planck Institute for Meteorology (MPI); the National Centre for Atmospheric Research (NCAR); and the Hadley Centre for Climate Prediction and Research, Met Office (UKMO).

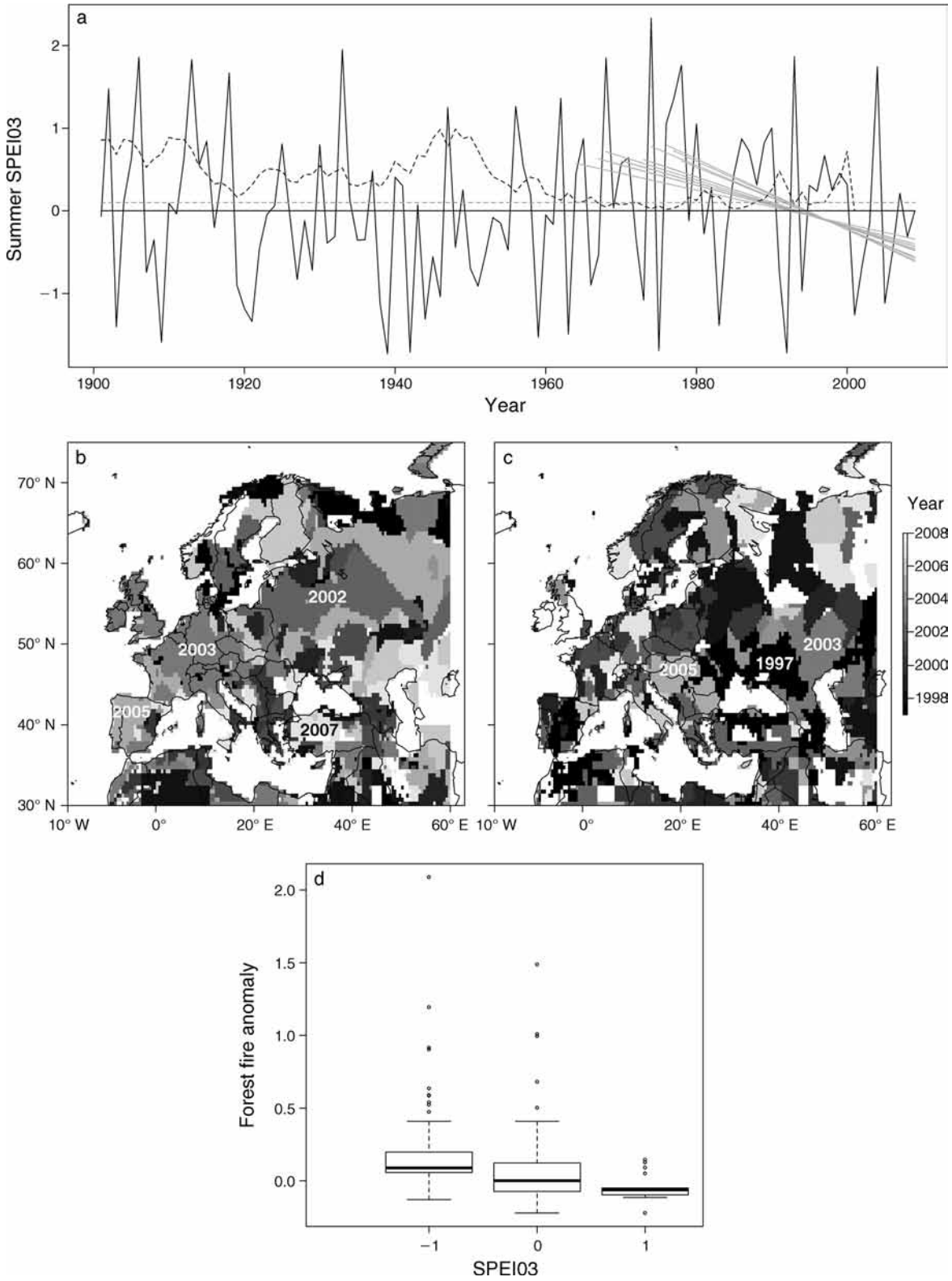

FIG. 4. (a) Summer SPEI03 (standardized precipitation–evapotranspiration index) time series for the 1900–2010 period in Chernobyl, Ukraine (black line). Annual *P* values (Mann-Kendall trend test) for the SPEI03 trend between 1969 and 2009 are also presented (dark gray, dashed line) with the 0.1 threshold (light gray, dashed line) and their respective linear interpolation (gray lines). Maps of European (b) minimum and (c) maximum summer SPEI03 years based on the SPEI03 months time frame for

trends until 2009, Fig. 4a), indicating that the summer periods became drier over time and suggesting an increasing trend in forest fire risk.

Fire activity and land cover

Accurate quantification of carbon and particulates emitted during fire events is significantly enhanced when land-cover types affected by fires are characterized. The presence of continuous and homogeneous patches is a key variable that allows fires to spread over large areas during extreme events (Cary et al. 2006). We explored the relationship between fire occurrence and land cover in Europe by using the tree cover map for Europe (Appendix: Fig. A1).

Fig. 5a illustrates the relationship between burned area and tree cover at the continental level. We observed that the largest burned area occurred in regions with tree cover less than 60%, mostly in the grassland steppes of Eastern Europe. However, although the mean burned area was low when tree cover exceeded 60%, the 95th percentile remained high for these areas. This finding indicated that large fires might occur over densely forested regions (potentially leading to extreme TC and TPM emissions, Appendix: Fig. A3) when fuel amounts and tree cover are high, although the average burned area appeared to be much lower. The continental-level distribution of the probability of fires to spread into dense forests was calculated by multiplying burned area by tree cover (Fig. 5b). Eastern Europe and Portugal were found to be the areas that were more prone to create fires in dense forests, including the contaminated forests of Ukraine and Belarus, potentially leading to high particulate emissions.

Because extreme forest fires also depend on the homogeneity and continuity of forest patches in order to spread, we computed largest patch index (LPI) and mean patch area (MPA) (Fig. 6a and b). The LPI identifies the percentage of area of a grid cell where contiguous forest pixels are aggregated into a single patch that could potentially spread a fire without any fuel breaks. MPA identifies the average size of forest patches, including LPI and other isolated forest patches. Boreal forests appeared as the most uniform forest areas for both indices, whereas forests in Southern Europe were more fragmented. However, large forest patches remain in Southern Europe, particularly around the Mediterranean basin and the mountainous areas. When landscape indices with burned area (BA) were combined (Fig. 6c and d) to gauge the probability of a fire spreading over large forest patches, we observed that Portugal and Ukraine were at the highest risk when considering LPI, and the temperate/boreal forests of

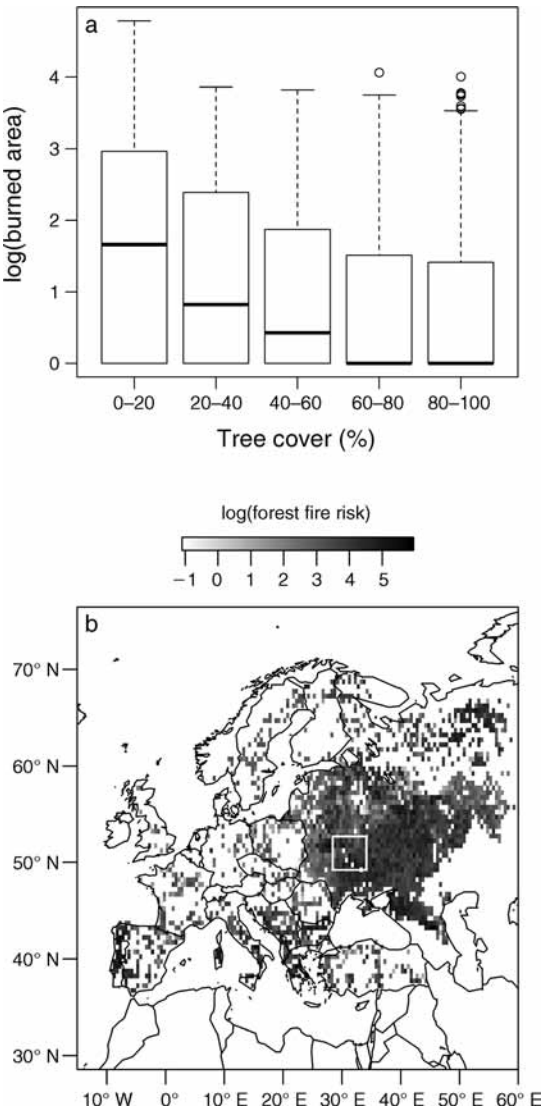

FIG. 5. (a) Box plot representing mean (center line), standard deviation (box edges), 95th percentile (whiskers), and outlier events (open circles) of burned areas (GFED3; measured in hectares) as a function of percent tree cover (Kempeeners et al. 2012). In general, burned areas were smaller in areas with high tree cover (pushing the median close to zero), although a few extreme events were recorded at high tree cover. These rare events, however, emitted a large amount of smoke with respect to the biomass consumed. (b) Forest fire risk as a result of a combination of burned area (BA, GFED3) and tree cover (data from Kempeeners et al. 2012) (calculated as percentage burned per hectare of tree cover). Large fires in dense forests are likely to happen in Ukraine and Portugal. The white square represents the area of our interest in Chernobyl and Belarus.

←
September from Vicente Serrano et al. (2012). (d) Box plot representing mean (center line), standard deviation (box edges), 95th percentile (whiskers), and outlier events (open circles) of burned area for the period 1997–2008 over Chernobyl vs. summer SPEI03 anomalies. Significantly higher burned areas occur during drier years (negative SPEI03).

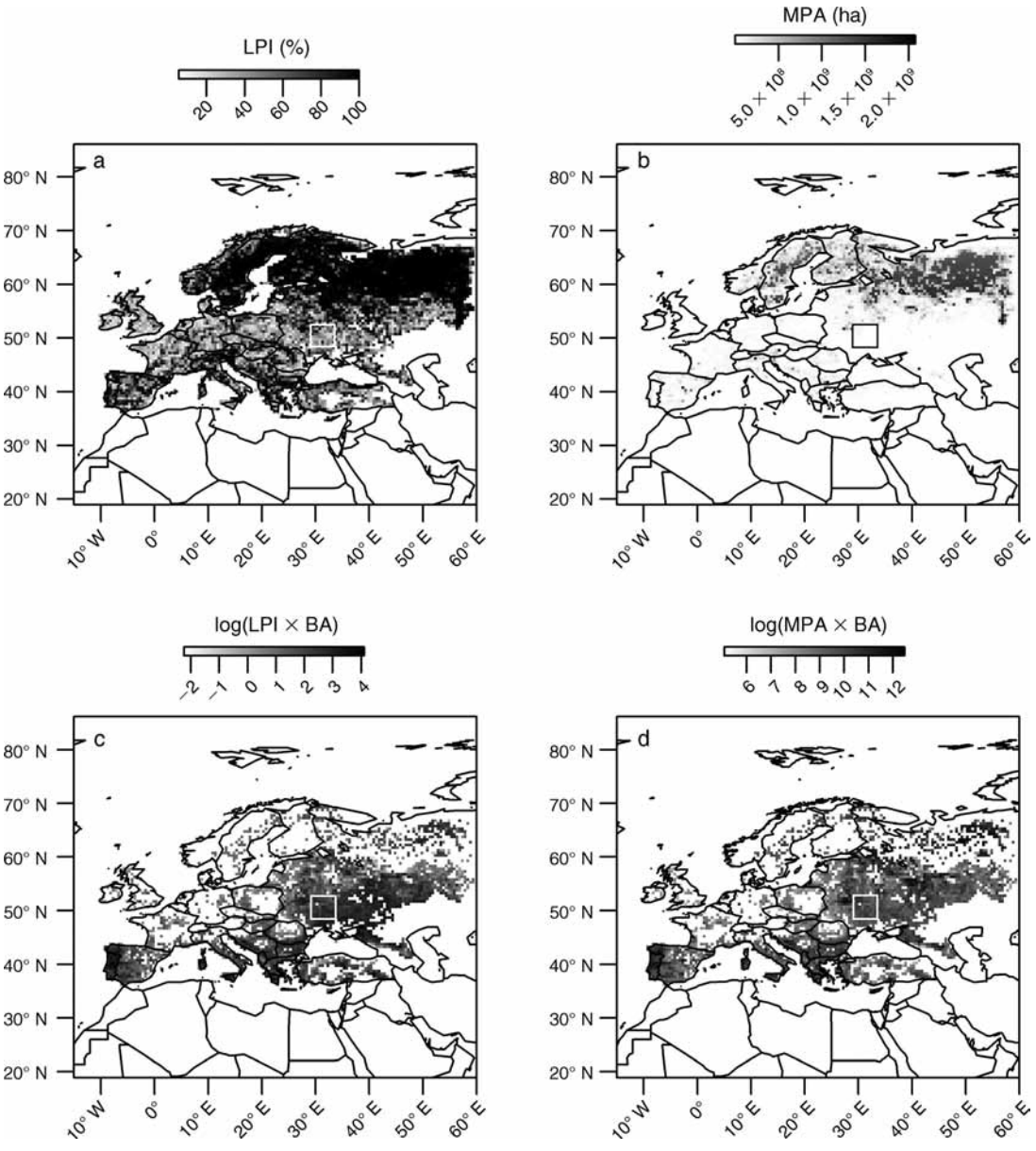

FIG. 6. Landscape analysis of forest patches based on a forest map derived from the Kempeeners et al. (2011) tree-cover map with a threshold of 50%. (a) Largest patch index (LPI, percentage of the grid cell) and (b) mean patch area (MPA, ha) are represented with their respective fire risks (c) LPI × BA (% per ha) and (d) MPA × BA (ha^2). The white (black in panel [b]) squares represent the area of our interest in Chernobyl and Belarus.

Russia were at the highest risk when considering MPA. This analysis indicated that Mediterranean and Eastern European forests, including Ukrainian and Belarusian forests, are highly prone to extremely large fire events that could produce large emissions of deposited radionuclides.

Since homogeneous landscape patterns (able to carry large fires) were found to contribute significantly to higher fire risk, changes in forest cover and in turn landscape structure within the ChNPP were assessed. Because the Chernobyl area has been protected from human activities since 1986, we expected that land-cover changes, including forest expansion or shrubby encroachment, would have happened in the last 25 years. To test this hypothesis, we analyzed and reclassified two Landsat images from winter 1987 and winter 2010 in which snow covered the ground but the canopy of trees; hence contrasts between croplands/grasslands and forests were highly visible and we could easily classify land cover as forested and non-forested. Fig. A4a in the Appendix represents land-cover changes between 1987 and 2010; we observed forest expansion north and west

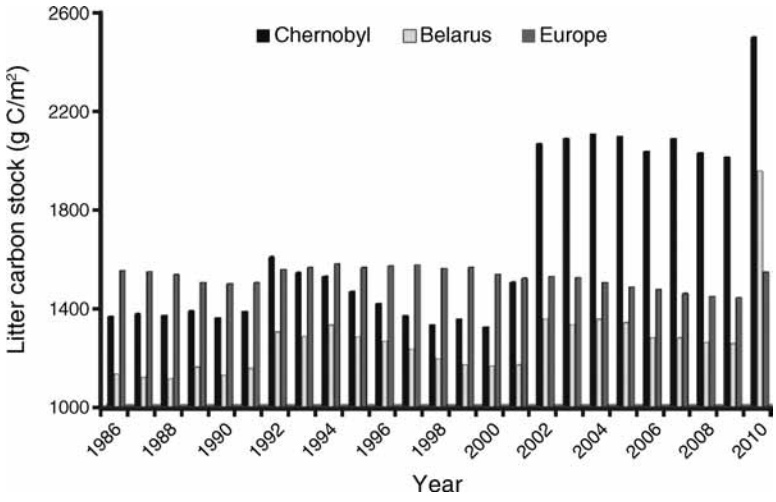

FIG. 7. Litter carbon stock for the period 1986–2010 centered in the Ukrainian (Chernobyl) and Belarusian contaminated forests.

of the ChNPP (+25%), characterized by a concomitant 10% increase in forest cover. This observation confirmed our hypothesis that forests were becoming less fragmented and thus potentially more capable of spreading large wildfires. Our local analysis was consistent with the recent analysis of global land-cover change by Hansen et al. (2013; Appendix: Fig. A4b), in which forest increase was the dominant pattern in the ChNPP exclusion zone during 2000–2012.

Biomass burning and litter carbon storage

Fig. A5 in the Appendix depicts biomass burning estimated by the PKU-FUEL model of Peking University for the years 1986 and 2007 in Europe. The year 1986 was chosen as a reference period just after the accident to show the large variability of the biomass consumption between the period of the accident and the present. Dancause et al. (2010) noted that a majority of people living in contaminated areas in Ukraine habitually burn stalks of potatoes during August–October, increasing the surface concentration of ^{137}Cs by almost a factor of 10. Moreover, most households outside cities are heated with firewood (77% of respondents in Rivne Oblast), and cooking is often done on wood-burning stoves (52%). Hence, the consumption of firewood has increased by a factor of 16 (0.02–0.33 kg·m^{-2}·yr^{-1}) in contaminated regions two decades after the Chernobyl disaster. Consumption of straw has also increased from 0.01 to 0.06 kg·m^{-2}·yr^{-1}, especially in Belarus. Farmers also light fires in their fields to burn weeds, potato stems, and other plant material; such fires can lead to uncontrolled forest fires. However, the MODIS active fires product showed no increase in agricultural fires up to 2007 because so few people live inside the contaminated areas of Ukraine and Belarus. Most fires in these areas were attributable to natural causes such as lightning.

The LPJmL-SPITFIRE model was used to estimate the variation of litter carbon stock in Europe since 1986. Litter carbon storage was plotted for the contaminated forests in Ukraine and Belarus (Fig. 7). Two main peaks in litter carbon stock were distinguished in Chernobyl, one in 1992 and the second in 2002, when litter carbon storage reached 2400g C/m^2. Litter carbon stock in Chernobyl has doubled since 1986 (particularly after 2000), which is likely due to the lack of any forest management in the area. Similar results were found for the forests of Belarus, with lower carbon stocks in general. The increase in accumulation was more pronounced in recent years with a notable peak in 2010 (1200–1850 g C·m^{-2}·yr^{-1}). These carbon stocks are very high compared to those observed elsewhere. For example, Averti and Dominique (2011) reported that litter carbon stock rates range between 1063 and 1824 g C·m^{-2}·yr^{-1} in Central Africa, whereas Raich et al. (2006) reported litter carbon stock rates in tropical forests as 700 g C·m^{-2}·yr^{-1}. However, those numbers are products of the rate of decomposition through heterotrophic respiration. In cold environments, reduced soil respiration leads to a build-up of carbon, in contrast to the fast-cycling tropics. Therefore, the most suitable comparison was with the data of Covington (1981), which is 1600 g C·m^{-2}·yr^{-1} for boreal forests generally; litter carbon stocks estimated for Ukrainian and Belarusian forests were thus relatively high.

A recent study of litter decomposition and storage in Chernobyl, however, suggests that our estimates of litter carbon stock are likely to be lower than those actually observed (Mousseau et al. 2014). The stock of litter carbon is a function of the annual amount of plant biomass in litterfall, minus the annual rate of decomposition. Litter mass is also influenced by the timing and types of disturbance influencing the forest. During the early stages of stand development, litter increases

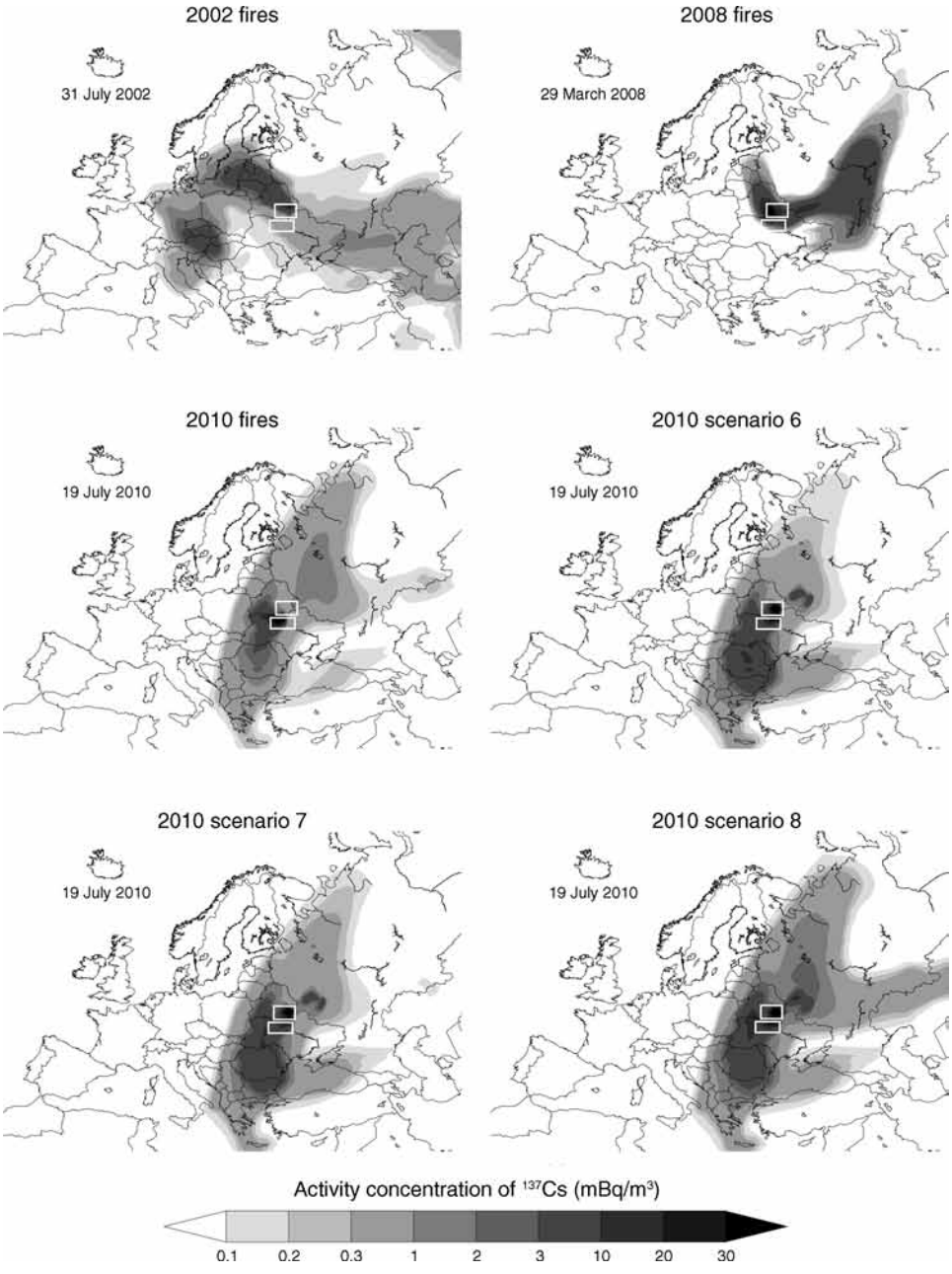

FIG. 8. Examples of ^{137}Cs emissions in the contaminated forests of Belarus and Ukraine after fire events in 2002, 2008, and 2010, as well as following the three different fire scenarios (2010 scenario 6, 2010 scenario 7, and 2010 scenario 8). The white boxes denote the location of the radioactive forests of Chernobyl (Ukraine) and Belarus.

rapidly. Management such as timber harvesting, slash burning, and site preparation dramatically alter litter properties (Fisher and Binkley 2000), but few studies clearly document the effects of management on litter carbon storage (Smith and Heath 2002).

Transport and deposition of ^{137}Cs after fires

Fires in Ukraine and Belarus were simulated for the years 2002, 2008, and 2010 using the LMDZORINCA model. MODIS satellite imagery recorded 185 fires in 2002, 50 in 2008, and 54 in 2010 that burned 473, 125, and 137 ha, respectively. The same 54 fire incidents in 2010 were used to simulate the three scenarios of fires occurring in 10% of the contaminated forests (2010 scenario 6, 2010 scenario 7, and 2010 scenario 8). Fig. 8 shows examples of some intense emissions during those years, in terms of activity concentrations of ^{137}Cs.

Several events in 2002 redistributed and transported ^{137}Cs over Europe. A major drought and prolonged high temperatures resulted in unprecedented fires. These fires

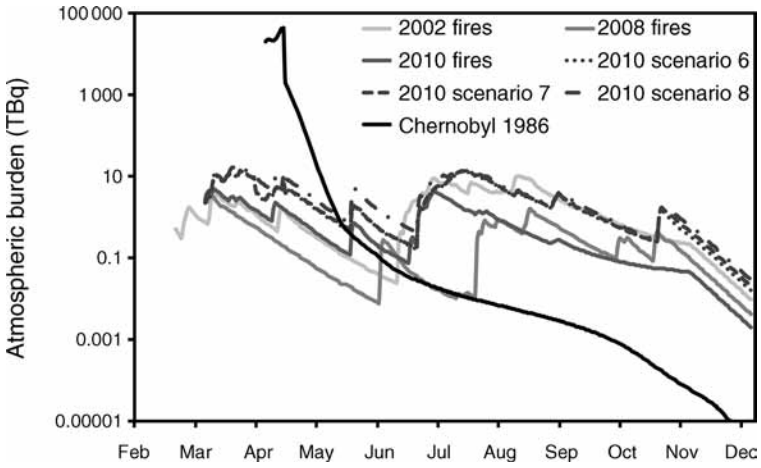

FIG. 9. Atmospheric burden of ^{137}Cs (TBq) after the fires in 2002, 2008, and 2010, as well as after the three fire scenarios with 10% of the area being burned (2010 scenario 6, 2010 scenario 7, and 2010 scenario 8). The respective burden from the Chernobyl accident in 1986 is shown in reference to the levels attained due to the fire events and the scenarios studied.

occurred under extreme fire danger conditions and were impossible for the authorities to extinguish. These fires were so serious that peat bogs also burned, followed by forests, causing massive smoke emissions that persisted for a period of nearly 2 months, sometimes reducing visibility to below 60 m. These fires resulted in significant exposures of smoke to major population centers such as Kiev and Moscow. The highest release occurred at the end of July, with ^{137}Cs fallout reaching Sweden, Finland, and Central Europe (Fig. 8).

Fires in 2008 were of lower intensity and frequency. However, some took place inside highly contaminated regions, injecting a significant plume into the atmosphere. In March 2008, ^{137}Cs covered Belarus and a large part of Russia (Fig. 8), and another event in August distributed ^{137}Cs more locally (data not shown).

Wildfires in 2010 affected several countries of Southern Europe, including the Balkan countries, Turkey, and southern Italy (Fig. 8). The same raging forest fires affected ~3900 ha locally in the fallout zone from the 1986 disaster. Despite the observed transport, it is noteworthy that the atmospheric activity concentrations of ^{137}Cs remained low (1–5 mBq/m^3).

The highest exposure to the radioactive cloud from the 2002, 2008, and 2010 fires occurred over Central Europe (Fig. 8), with an annual average air activity concentration of ^{137}Cs ranging from 17 to 120 mBq/m^3, whereas the maximum displacement of ^{137}Cs was estimated to be only four orders of magnitude lower than the initial total deposition in 1986 (85 PBq; De Cort et al. 1998). In the three scenarios (2010 scenario 6, 2010 scenario 7, and 2010 scenario 8), 10% of the contaminated forests in Chernobyl and Belarus were burned (using the temporal pattern of 2010 wildfires, as recorded from MODIS and accounting for a maximum injection height of 2.9, 4.3, and 6.0 km, respectively). As the altitude of the release increased, the plume spread and therefore covered a larger surface area (Fig. 8). Nevertheless, the transport was not significantly different whether ^{137}Cs was released at 2.9 or 6.0 km, likely because we accounted for a small emission factor of ^{137}Cs after fires (40%) and/or because the highest releases occurred during summer when surface winds are relatively weak and do not favor advection. Fig. 9 depicts the atmospheric burden of ^{137}Cs as a time series for the simulated period (March to December), and indicates that if fires burned 10% of the areas, an enormous amount of ^{137}Cs would be released. In 2002, when according to MODIS, intense fires were burning for almost two months inside highly contaminated areas, fire emissions fell within the same range as the scenarios (that is, more than 8% of ^{137}Cs remaining from Chernobyl was released). Differences in the amount of ^{137}Cs that remained in the ambient aerosol and was finally transported for longer time periods were due to the different injection heights used in each scenario. The lifetime of ^{137}Cs in the atmosphere was calculated as ~5 days, which conforms with many other studies.

The deposition of ^{137}Cs was larger in 2002 compared to the other years (2008 and 2010). ^{137}Cs migrated to the south, affecting the Kiev metropolitan area as well as Romania and Bulgaria (Fig. 10), although the concentrations were low and likely presented a small radiological hazard. The trend of ^{137}Cs migration to the south has been verified by measurements of soil concentrations in Ukraine during the last 25 years presented in the atlas of radioactive contamination of Ukraine (NRU 2011). Aside from fires, horizontal migration of ^{137}Cs may occur due to rain, snow melt, and human activities including traffic, street washing, and cleanup, in which radionuclides are washed from surfaces and transported within settlements, some being removed with litter and sewage. One of the consequences of these processes has been secondary contamination of sewage systems and

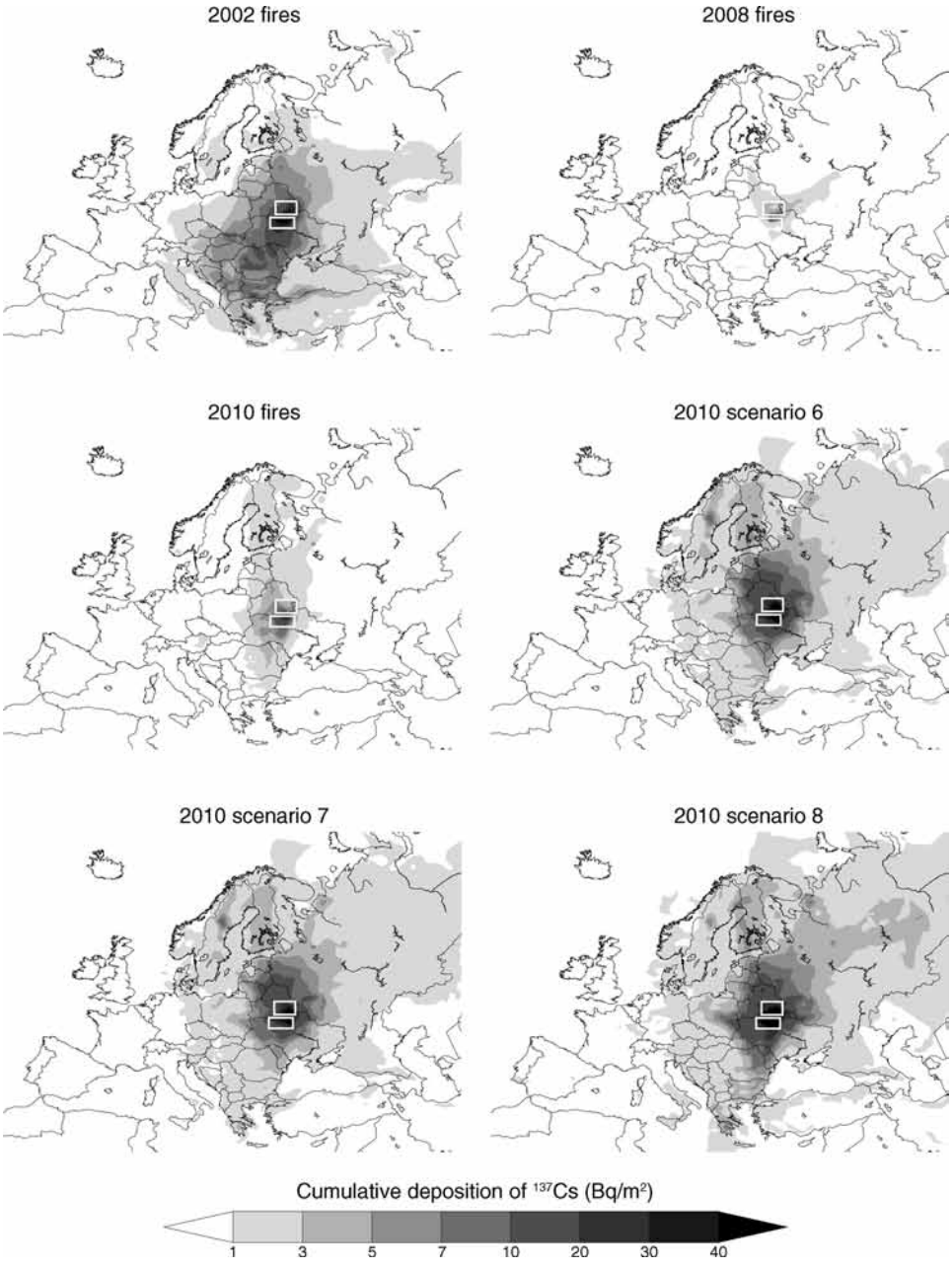

FIG. 10. Deposition of ^{137}Cs (wet and dry) after fires in 2002, 2008, and 2010 in Ukraine and Belarus, as well as during the three scenarios studied (2010 scenario 6, 2010 scenario 7, and 2010 scenario 8). Values present cumulative deposition of ^{137}Cs integrated to the end of each of the studied years. The white boxes denote the location of the radioactive forests of Chernobyl (Ukraine) and Belarus.

sludge storage, which necessitates special cleanup measures.

In general, ^{137}Cs has not been transferred at large concentrations to large urban areas yet. Our simulations showed that 32.2, 7.2, and 9.6 kBq/m^2 of ^{137}Cs were deposited after the fires in 2002, 2008, and 2010, respectively, whereas the three scenarios predicted that >40 kBq/m^2 of ^{137}Cs would be deposited over Europe. The maximum atmospheric dispersion of ^{137}Cs after all the simulations corresponded to almost 8% of what has been deposited on the area after the Chernobyl accident, corrected with an effective half-life of 10 years to 1 March of the years studied and almost 0.1‰ of the core inventory of Reactor 4 of ChNPP that exploded on 26 April 1986. Thus, deposition would contribute 1–10 μSv/yr to the total effective dose of an inhabitant in Kiev.

Discussion

Several models, together with remote-sensing data and direct observations, are employed here for the first time to provide the first realistic analyses of past and present trends and risks of forest fires in the radioactively contaminated forests of Ukraine and Belarus. We also issue future predictions of fire incidents. The results show that temperatures in the contaminated forests are expected to increase in the future, whereas precipitation will remain the same or decrease slightly. These changes have important policy implications for the risk of fire and for fire management.

Roles of vegetation in promoting the risk of fire

Worldwide, somewhere between 75 and 820 million hectares of land burn each year, depending on the year. Wildfires (not including fires intentionally set to clear land) consume some 3–8% of total terrestrial net primary productivity annually, releasing on average 1.7–4.1 Gt of carbon into the atmosphere (van der Werf et al. 2010). There is a growing realization that climate change may be associated with increasing forest fire size, frequency, and severity (in terms of the number of trees killed) across boreal and sub-boreal regions (Westerling et al. 2006, Williams et al. 2013), despite widespread management practices aimed at reducing flammable materials in forests. Climate models predict that higher temperatures and longer droughts will increase wildfire frequency, particularly in semiarid regions. Fig. 2 shows that temperature will continue to increase in coming years in Chernobyl and Belarus, and the average annual air temperature will have reached 14°C by 2100. Higher rainfall in some areas could reduce fire frequency, though it could also foster more vegetation, thus providing more fuel for fires. Lightning (an important ignition source) is thought to increase with a warmer climate, and more intense rainstorms could exacerbate post-fire runoff and landslides.

Warming trends also may already be contributing to increasing stress on boreal forests such as those that predominate in the Chernobyl region. Warming can increase tree stress by increasing water deficit and thus drought stress on trees (McDowell et al. 2008) and/or enhancing the growth and reproduction of insects and pathogens that attack trees (Raffa et al. 2008). Indeed, a major insect outbreak occurred in Chernobyl in summer 2011, leaving a large swath of forest with completely defoliated trees. Recent episodes of forest dieback (Breshears et al. 2005, Williams et al. 2013) and rising tree mortality rates in otherwise undisturbed forests (van Mantgem and Stephenson 2007) may also be due to stress from warming climate. Trees subject to chronic water and/or temperature stress are more sensitive to subsequent fire damage (van Mantgem et al. 2003), implying that recent warming trends may lead to a de facto increase in fire severity, apart from changes that may increase fire intensity.

Vegetation type distribution, interannual variation in amount of fuel and fuel moisture content, and landscape patterns affect fuel continuity and the capacity of a fire to crown and spread. We explored these constraints and their trends throughout Europe and at local scales in Chernobyl and Belarus. The relationship between extreme fire years and increasing frequencies of summer drought will potentially result in larger burned areas. Grassland fields appear to be the most fire-prone areas in Europe. When burned area is combined with tree cover, the Mediterranean and Eastern Europe (including the contaminated forests in Ukraine and Belarus) emerge as the major regions with forests threatened by fires. Extreme fire events are likely to occur over large, contiguous forest patches; since these regions exhibit both high fire occurrence and large forest patches, we conclude that extreme fire events will likely occur there. These forests extend up to the interface between large boreal forests (which show low fire activity due to limited drought) and up to fragmented, fire-prone areas of Southern Europe (which show lower risks of large fires). Local-scale analysis illustrated the significant forest cover gains around the ChNPP since 1986, suggesting an increasing continuity in forest patches and, in turn, higher fire risk.

Accumulation and loss of carbon litter stocks

In boreal forests generally, the rate of decomposition is slower and leads to the accumulation of a thick litter layer, also known as a mor (Schlesinger 1997). Another source of variability of litter storage is caused by tree mortality. Widespread forest dieback due to increasing drought or heat stress as well as post-fire mortality can lead to short-term carbon inputs to the litter pool that exceed annual inputs from leaf and root turnover. This is exactly what the LPJmL-SPITFIRE predicts for the Chernobyl and Belarusian forests shown in Fig. A6 of the Appendix. Litter carbon stock in the contaminated forests has increased since 1986, with a major peak in 2010 due to the lack of forest management. Thereafter, carbon litter stocks in Belarus and Ukraine decrease to half by 2030 (compared to 2010), interrupted by a rapid peak in 2035, whereas average litter carbon in Europe (as a whole) remains at the same level (Fig. 11). However, the situation in the contaminated areas changes after 2060, when litter carbon storage in Belarus reaches a maximum after having increased around 2.5 times since 1986 (Fig. 7 and Appendix: Fig. A6). The same trend is observed in Chernobyl, with litter carbon increasing by a factor of 2 after 1986 reaching the 2010 values ($\sim$2400 g C/m^2). According to the LPJmL-SPITFIRE model, litter carbon stocks in Chernobyl and Belarus gradually decrease again after 2070, as they are probably consumed by increasing

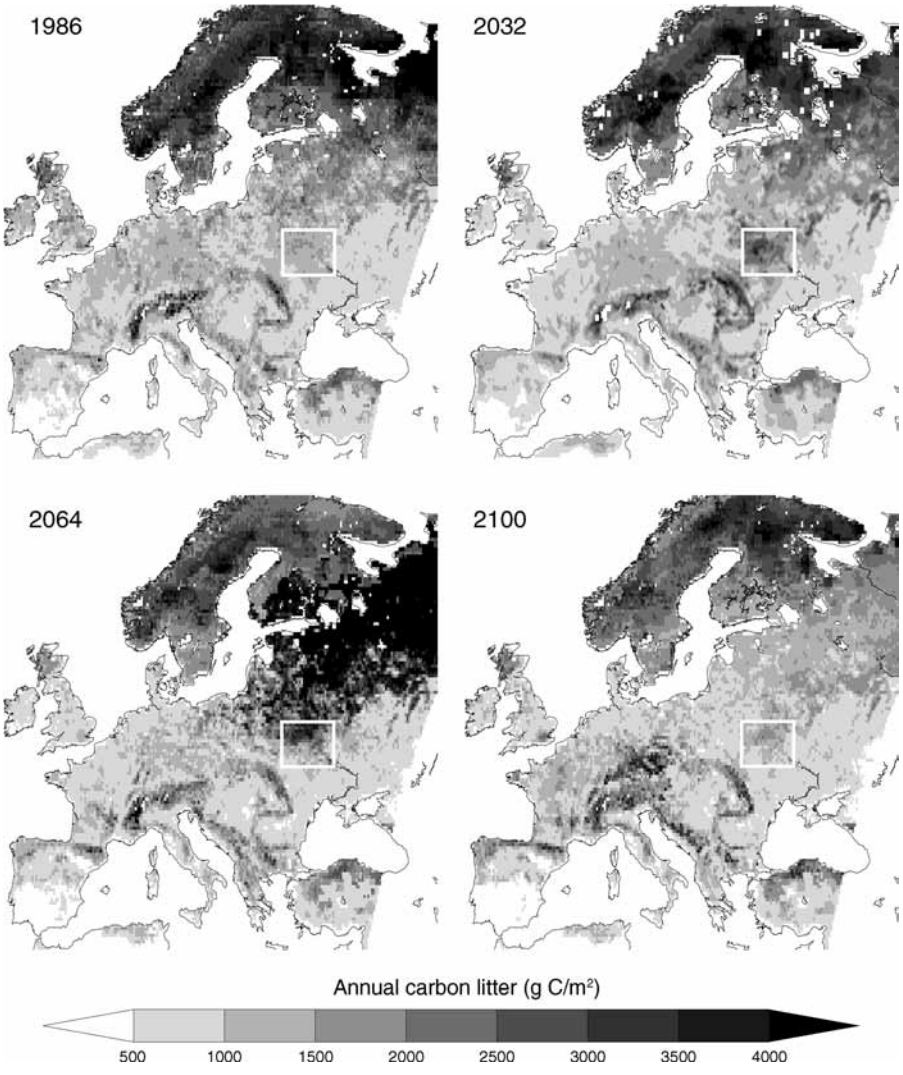

FIG. 11. Litter carbon stock over Europe 1986–2100 based on the future prediction of the LPJmL-SPITFIRE model. White rectangle denotes the contaminated forests in Ukraine and Belarus.

numbers of fires during the same period (Appendix: Fig. A6).

These effects may be further exacerbated in contaminated regions by the influence of radiation on decomposition and tree growth in the Chernobyl region (Mousseau et al. 2013, 2014). Radioactive contamination impedes decomposition rates of organic matter due to its negative effects on soil biota. Background radioactivity has reduced the rate of decomposition of plant material in large areas around Chernobyl (Fig. 12). When leaf litter collected in uncontaminated areas, far south of the exclusion zone, is placed inside highly contaminated areas, the decomposition rate in contaminated areas is only one-half of that recorded for similar types of leaf litter in control areas (Mousseau et al. 2014). As a consequence, the litter layer in the most contaminated areas is now four times thicker than that in the least contaminated areas around Chernobyl (Mousseau et al. 2014). The predicted litter carbon stock likely significantly underestimates the potential hazards related to litter amount in these forests. Clearly, such large differences in the amount of dead plant material can have radical consequences for the risk of fire and the magnitude of fires once an ignition has occurred.

Surface detritus facilitates the capture and infiltration of rainwater into lower soil layers and its removal by fire accelerates soil erosion (Chanasyk et al. 2003). In addition, soil litter reduces wind erosion by preventing soil from losing moisture and providing cover preventing soil transportation. Organic matter accumulation also helps to protect soils from wildfire damage. Standing vegetation can be severely reduced and soil litter almost completely removed depending on the

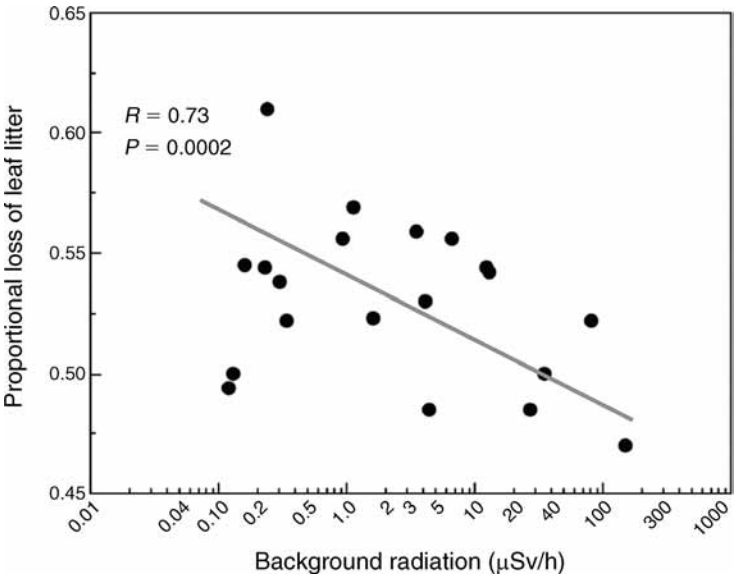

FIG. 12. Proportional loss (decomposition) of leaf litter from leaf litter bags containing uncontaminated leaf litter and placed in the litter layer at 20 different sites around Chernobyl during a nine-month period in relation to background radiation level (note log scale of *x*-axis).

intensity and severity of wildfires and season (Ice et al. 2004).

Radionuclide releases from fires

The largest radionuclide release to date occurred in 2002, when fires in contaminated regions burned for almost 2 months. However, low radionuclide concentrations were recorded (on the order of 1–5 mBq/m^3), and mostly affected the local population. It seems that ^{137}Cs migrates to the south with time as a result of fires, washout, and human activities. The amount of ^{137}Cs redeposited over Europe has been equivalent to 8% of what was deposited following the initial disaster, which is relatively low compared to the total amount of ^{137}Cs available in these forests.

It should be stated here that ^{137}Cs redistribution is not the only problem after a fire event in the Ukrainian and Belarusian forests. Thirteen of 19 radionuclides, released in the range of PBq in 1986, exhibit half-lives from a few days to 2 years, meaning that they have been lost due to decay. However, of the remaining radionuclides, four of six are refractory, long-lived elements ($^{238–240}$Pu and traces of ^{241}Am) that have been "trapped" in the CEZ, whereas the other two (^{137}Cs and ^{90}Sr) are volatile elements with half-lives of about 29 and 30 years. According to measurements (NRU 2011) and our simulations (assuming an effective half-life of 10 years), we estimate that 2–8 PBq of ^{137}Cs and 1–4 PBq of ^{90}Sr still remain in the contaminated areas of Ukraine and Belarus, whereas the rest ($^{238–240}$Pu and traces of ^{241}Am) are in the order of TBq. In addition, approximately one-quarter of the total amount of radionuclides from Chernobyl was deposited in southwestern Russia next to the Ukrainian-Belarusian borders. These parts of Russia have similar habitats and climate to the contaminated forests of Ukraine and Belarus. However, for logistical reasons, we were unable to obtain sufficiently detailed information for Russia. Hence, the magnitude of the effects that we have documented here clearly underestimates the combined effects predicted for all contaminated areas.

Firefighting and policy changes in contaminated forests

Increased fire risk in these forests and the subsequent release of radionuclides are exacerbated by the lack of firefighting infrastructure in the contaminated zone. Despite political pronouncements, a lack of financial resources impedes the implementation of policies that have been adopted to date. Although some promising actions have been introduced by international organizations, renewal of the fire crew and modernization of the firefighting equipment are both required to combat the risk of a major fire event.

Since 1991, when the Ukrainian Law "About legal status of the territory that was contaminated by radionuclides as a result of the Chernobyl disaster" was adopted by the Parliament of Ukraine, the main objective of the fire policy has been to keep the territory in "fire safe condition." Fire prevention was recently emphasized as a priority in the Order of the Cabinet of Ministers of Ukraine (p. 535, 18.07.2012, "Concept of implementation of state policy in a sphere of development of activity in certain zones of radioactive contamination due to Chernobyl catastrophe").

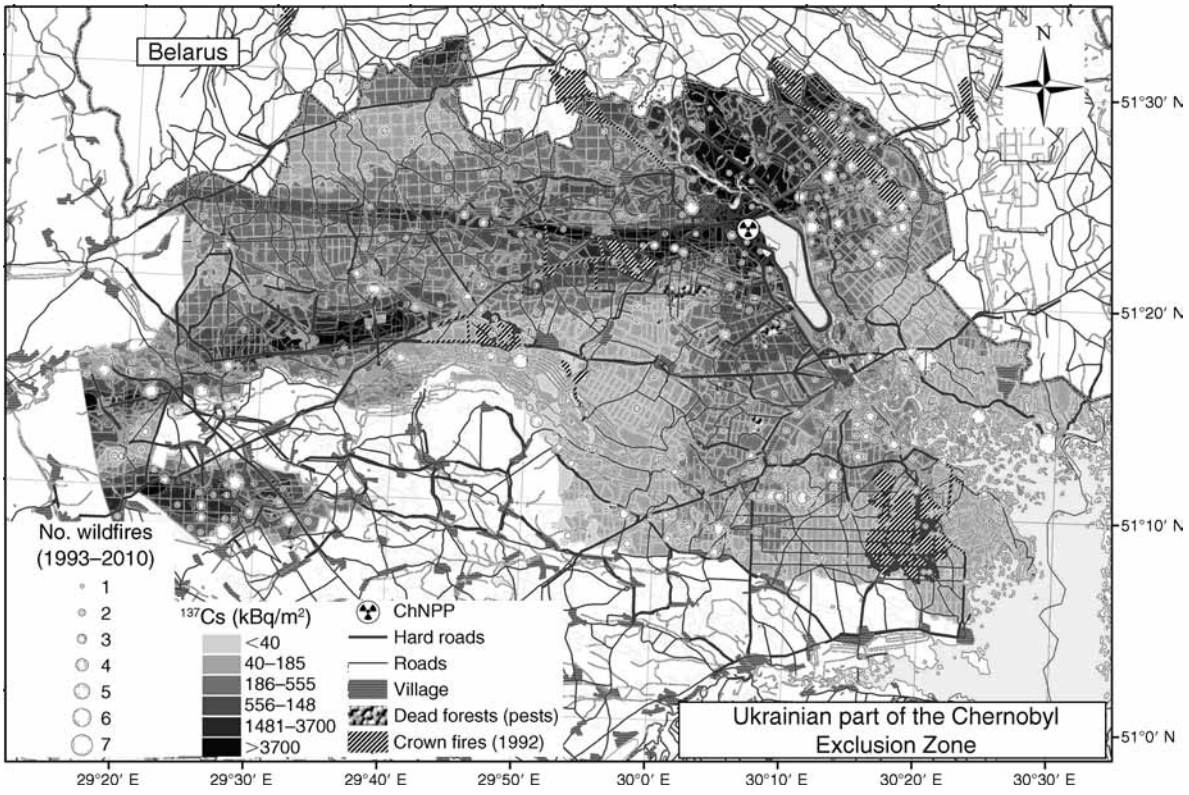

FIG. 13. Wildfire history in the Chernobyl Exclusion Zone (CEZ).

With an emphasis on prevention, firefighting capacities have not been given enough attention in the area. During 1986–1992, professional firefighters at the Chernobyl Fire Station were responsible for forest firefighting; however, in practice, this staff was mainly trained for suppressing infrastructural fires, not wildfires. The absence of the basic components of forest fire management in CEZ, such as prevention, fire detection, early warning, and a cogent fire management plan, led to a series of catastrophic wildfires in August 1992 that burned ~17 000 ha of contaminated land, including 5000 ha due to a massive crown fire in Opachichi forest district. As a result, a special forestry enterprise, Chornobyl Forest, was established in the CEZ in 1992, with 600 professional forestry staff focused on implementing a forest fire management system.

Despite some success in terms of preventing catastrophic fires during 1993–2010, fire risk and fire hazard have been increasing steadily in the CEZ. Ignition sources are present throughout the territory of the CEZ during the entire fire season as construction of the second sarcophagus proceeds and returning villagers, CEZ staff, and illegal visitors conduct agricultural burns. According to official statistics, ~1100 small and medium size wildfires occurred during 1993–2010 in CEZ, including the most contaminated zones (Zibtsev et al. 2011) (Fig. 13).

Fire management has deteriorated during the past decade due to a dearth of funding and the attendant lack of specific policy laws and administrative efforts. Chornobyl Forest staff, including firefighters, has been cut by almost 40% over the past two decades. The existing fire detection system, consisting of six lookout towers, covers only 30–40% of the CEZ, and half of the wildfires usually occur outside its detection radius (Fig. 13). Most of the heavy firefighting equipment is at least 10 years old, outdated, and not reliable in dealing with fire emergencies. The number of fire stations (four), fire crews, and engines per 1000 ha of forest are six to seven times fewer than those of normal forest stations in Ukraine outside of the CEZ (Fig. 14). Only ~20–30% of the required prevention measures in the CEZ are executed annually due to lack of funding and the dramatic reduction of the forest road network available for fire engines. Thus, there are many parts of the CEZ that are practically unreachable by firefighters.

Steps forward to improve forest safety should start with the employment of fire crew personnel who will execute the prevention measures and take part in the firefighting process. In reaction to the current situation and the subsequent concern of international organizations (e.g., the United Nations, U.S. Forest Service, and Organization for Security and Co-operation in

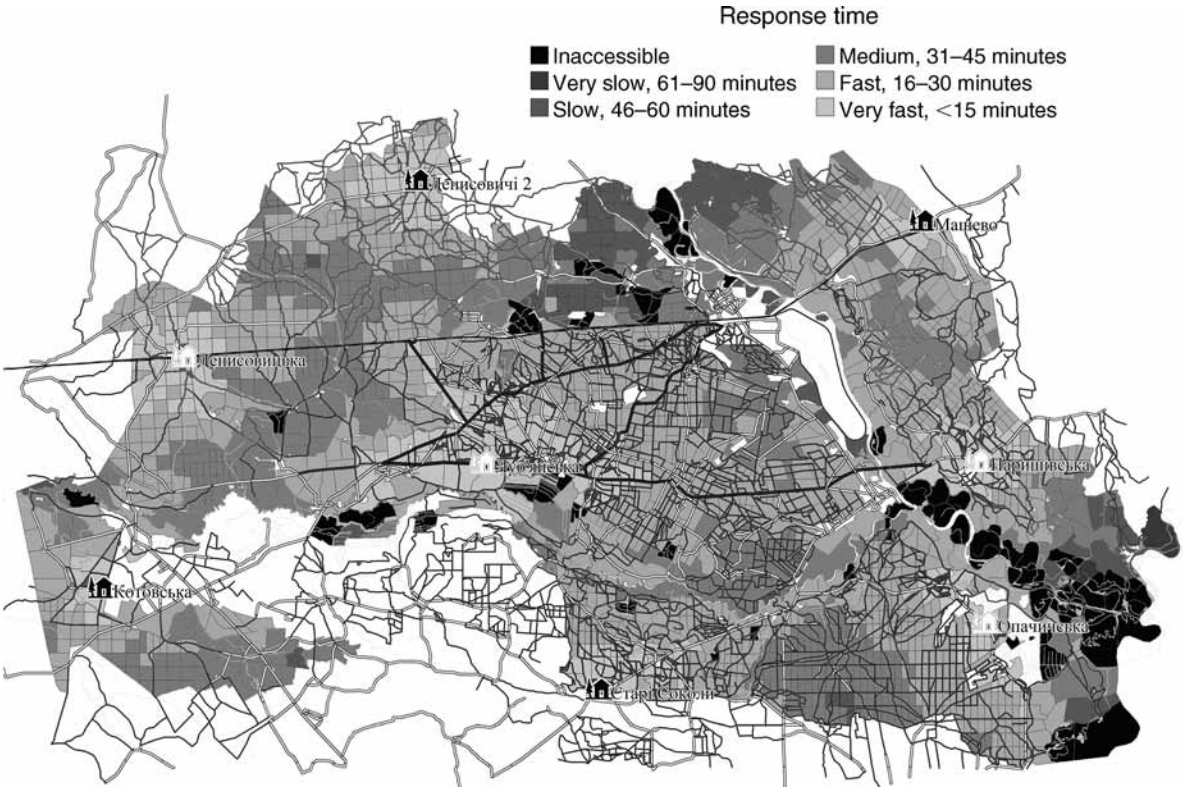

FIG. 14. Zones with different response times needed for fire crews to reach certain parts of CEZ in case of fire. Lack of forest roads can delay responses. The four black buildings north, south, west, and east denote the available fire stations; the white buildings denote fire observatories. Shades of gray denote response time to access each forest area within CEZ.

Europe), the Government of Ukraine, UNEP (United Nations Environment Program), and other donors have recently initiated measures to improve the situation and decrease fire risk by developing a fire management plan and installing a video surveillance system that will cover the CEZ and neighboring territories outside of the zone. This system is expected to enable specialists to detect fires on monitors under safe radiological conditions, to conduct fire risk assessments, and to develop and run fire behavior models. Finally, early warning systems will be installed in order to inform the personnel of high radiation levels, thus preventing unnecessary exposure to radioactive contaminants.

ACKNOWLEDGMENTS

The authors are greatly appreciative of funding from the project GIS Climat-Environnement-Société, which supported the workshop entitled "Role of fire ignition in climate change and its relation to the redistribution of atmospheric constituents" (CNRS Campus, Gif-sur-Yvette, France, 23–26 October 2012). During this workshop, international experts on fire modeling, radioecology, and atmospheric science (the authors of the present paper) were gathered and discussed how to further develop and improve their models. The feedback of this workshop is incorporated into this paper. J. W. Kaiser was funded by the European Commission through the FP7 project MACC-II, contract number 283576.

LITERATURE CITED

Akagi, S. K., R. J. Yokelson, C. Wiedinmyer, M. J. Alvarado, J. S. Reid, T. Karl, J. D. Crounse, and P. O. Wennberg. 2011. Emission factors for open and domestic biomass burning for use in atmospheric models. Atmospheric Chemistry and Physics 11:4039–4072.

Amiro, B. D., S. C. Sheppard, F. L. Johnston, W. G. Evenden, and D. R. Harris. 1996. Burning radionuclide question: What happens to iodine, cesium and chlorine in biomass fires? Science of the Total Environment 187:93–103.

Averti, I., and N. Dominique. 2011. Litterfall, accumulation and decomposition in forest groves established on savannah in the Plateau Teke, Central Africa. Journal of Environmental Science and Technology 4:601–610.

Avery, S. V. 1996. Fate of caesium in the environment: distribution between the abiotic and biotic components of aquatic and terrestrial ecosystems. Journal of Environmental Radioactivity 30:139–171.

Bergan, T. D. 2000. Ecological half-lives of radioactive elements in semi-natural systems. NKS(97)FR5, ISBN 87-7893-025-1.

Bertschi, I. T., D. A. Jaffe, L. Jaeglé, H. U. Price, and J. B. Dennison. 2004. PHOBEA/ITCT 2002 airborne observations of trans-Pacific transport of ozone, CO, VOCs, and aerosols to the Northeast Pacific: Impacts of Asian anthropogenic and Siberian boreal fire emissions. Journal of Geophysical Research. http://dx.doi.org/10.1029/2003JD004200

Bondeau, A., P. C. Smith, S. Zaehle, S. Schaphoff, W. Lucht, W. Cramer, and D. Gerten. 2007. Modelling the role of agriculture for the 20th century global terrestrial carbon balance. Global Change Biology 13:679–706.

Breshears, D. D., et al. 2005. Regional vegetation die-off in response to global-change-type drought. Proceedings of the National Academy of Sciences USA 102:15144–15148.

Bunzl, K., and W. Kracke. 1984. The distribution of lead-210, polonium-210, stable lead and fallout caesium-137 in soil, plants and moorland sheep of a heath. Science of the Total Environment 39:143–160.

Cary, G. J., R. E. Kean, R. H. Gardner, S. Lavorel, M. Flannigan, I. D. Davies, C. Li, J. M. Lenihan, T. S. Rupp, and F. Mouillot. 2006. Comparison of the sensitivity of landscape fire succession models to variations in terrain, fuel pattern, climate and weather. Landscape Ecology 21:121–137.

Chanasyk, D. S., I. R. Whitson, E. Mapfumo, J. M. Burke, and E. E. Prepas. 2003. The impacts of forest harvest and wildfire on soils and hydrology in temperate forests: a baseline to develop hypotheses for the boreal plain. Journal of Environmental Engineering and Science 2:S51–S62.

Chin, M., P. Ginoux, S. Kinne, O. Torres, B. Holben, B. N. Duncan, R. V. Martin, J. A. Logan, A. Higurashi, and T. Nakajima. 2002. Tropospheric aerosol optical thickness from the GOCART model and comparisons with satellite and sunphotometer measurements. Journal of Atmospheric Science 59:461–483.

Cofer, W. R., E. L. Winstead, B. J. Stocks, L. W. Overbay, J. G. Goldammer, D. R. Cahoon, and J. S. Levine. 1996. Emissions from boreal forest fires: Are the atmospheric impacts underestimated? Pages 834–839 *in* J. S. Levine, editor. Biomass burning and global change. MIT Press, Cambridge, Massachusetts, USA.

Covington, W. W. 1981. Changes in forest floor organic-matter and nutrient content following clear cutting in Northern Hardwoods. Ecology 62:41–48.

Dancause, K. N., L. Yevtushok, S. Lapchenko, I. Shumlyansky, G. Shevchenko, W. Wertelecki, and R. M. Garruto. 2010. Chronic radiation exposure in the Rivne-Polissia region of Ukraine: Implications for birth defects. American Journal of Human Biology 22:667–674.

De Brouwer, S., Y. Thiry, and C. Myttenaere. 1994. Availability and fixation of radiocaesium in a forest brown acid soil. Science of the Total Environment 143:183–191.

De Cort, M., et al. 1998. Atlas of caesium deposition on Europe after the Chernobyl accident. Office for Official Publications of the European Communities, EUR 16733, Luxembourg.

European Centre for Medium-range Weather Forecasts (ECMWF). 2002. ERA-40, forty-year European re-analysis of the global atmosphere. http://www.ecmwf.int/products/data/archive/descriptions/e4

Evangeliou, N., Y. Balkanski, A. Cozic, and A. P. Møller. 2013. Simulations of the transport and deposition of ^{137}Cs over Europe after the Chernobyl NPP accident: Influence of varying emission-altitude and model horizontal and vertical resolution. Atmospheric Chemistry and Physics 13:7183–7198.

Filipovic-Vincekovic, N., D. Barisic, N. Masic, and S. Lulic. 1991. Distribution of fallout radionuclides through soil surface layer. Journal of Radioanalytical and Nuclear Chemistry Archives 148:53–62.

Fisher, R. F., and D. Binkley. 2000. Ecology and management of forest soils. Third edition. Wiley, New York, New York, USA.

Food and Agriculture Organization of the United Nations (FAO). 2013. Statistics at FAO. http://faostat.fao.org/site/291/default.aspx

Freitas, S. R., K. M. Longo, R. Chatfield, D. Latham, M. A. F. Silva Dias, M. O. Andreae, E. Prins, J. C. Santos, R. Gielow, and J. A. Carvalho, Jr. 2007. Including the sub-grid scale plume rise of vegetation fires in low resolution atmospheric transport models. Atmospheric Chemistry and Physics 7:3385–3398.

Freitas, S. R., K. M. Longo, J. Trentmann, and D. Latham. 2010. Technical Note: Sensitivity of 1-D smoke plume rise models to the inclusion of environmental wind drag. Atmospheric Chemistry and Physics 10:585–594.

Fromm, M. D., and R. Servranckx. 2003. Transport of fire smoke above the tropopause by supercell convection. Geophysical Research Letters 30:1542.

Fromm, M., O. Torres, D. Diner, D. Lindsey, B. Vant Hull, R. Servranckx, E. P. Shettle, and Z. Li. 2008. Stratospheric impact of the Chisholm pyrocumulonimbus eruption: 1. Earth-viewing satellite perspective. Journal of Geophysical Research 113:D08202. http://dx.doi.org/10.1029/2007JD009153

Gerten, D., S. Schaphoff, U. Haberlandt, W. Lucht, and S. Sitch. 2004. Terrestrial vegetation and water balance—hydrological evaluation of a dynamic global vegetation model. Journal of Hydrology 286:249–270.

Giglio, L., J. T. Randerson, G. R. van der Werf, P. S. Kasibhatla, G. J. Collatz, D. C. Morton, and R. S. DeFries. 2010. Assessing variability and long-term trends in burned area by merging multiple satellite fire products. Biogeosciences 7:1171–1186.

Hansen, M. C., et al. 2013. High resolution global maps of 21st century forest cover change. Science 342:850–853.

Hao, W. M., O. O. Bondarenko, S. Zibtsev, and D. Hutton. 2009. Vegetation fires, smoke emissions, and dispersion of radionuclides in the Chernobyl Exclusion Zone. Pages 265–275 *in* A. Bytnerowicz, M. J. Arbaugh, A. R. Riebau, and C. Andersen, editors. Developments in environmental science. Volume 8. Elsevier, Amsterdam, The Netherlands.

Hashimoto, S., S. Ugawa, K. Nanko, and K. Shichi. 2012. The total amounts of radioactively contaminated materials in forests in Fukushima. Japanese Scientific Reports. http://dx.doi.org/10.1038/srep00416

Hessl, A. E., D. McKenzie, and R. Schellhaas. 2004. Drought and Pacific decadal oscillation linked to fire occurrence in the inland Pacific Northwest. Ecological Applications 14:425–442.

Horrill, A. D., V. H. Kennedy, I. S. Paterson, and G. M. McGowan. 1995. The effect of heather burning on the transfer of radiocaesium to smoke and the solubility of radiocaesium associated with different types of heather ash. Journal of Environmental Radioactivity 29:1–10.

Hourdin, F., and J. P. Issartel. 2000. Sub-surface nuclear tests monitoring through the CTBT xenon network. Geophysical Research Letters 27:2245–2248.

Ice, G. G., D. G. Neary, and P. W. Adams. 2004. Effects of wildfire on soils and watershed processes. Journal of Forestry 102:16–20.

International Atomic Energy Agency (IAEA). 2001. Present and future environmental impact of the Chernobyl accident. IAEA, Vienna, Austria.

International Atomic Energy Agency (IAEA). 2005. Regulations for the safe transport of radioactive material. IAEA, Vienna, Austria.

International Atomic Energy Agency (IAEA). 2006. Chernobyl's legacy: health, environmental and socio-economic impacts and recommendations to the governments of Belarus, the Russian Federation and Ukraine. The Chernobyl forum: 2003–2005. Second revised version. IAEA, Vienna, Austria. http://www.iaea.org/Publications/Booklets/Chernobyl/chernobyl.pdf

International Atomic Energy Agency (IAEA). 2009. Regulations for the safe transport of radioactive material. IAEA, Vienna, Austria.

International Energy Agency (IEA). 2013. World energy statistics and balances. http://www.oecd-ilibrary.org/statistics

International Radioecology Laboratory (IRL). 2013. Radioecology research of the Red Forest Proving Ground, Kyiv, Ukraine. International Radioecology Laboratory, Chernobyl Center for Nuclear Safety, Radioactive Waste and Radioecology. http://www.chornobyl.net/en/index.php?newsid=1174890890

Joint Research Centre (JRC). 2014. EFFIS—European Forest Fire Information System. http://forest.jrc.ec.europa.eu/effis/applications/fire-history/

Kahn, R. A., Y. Chen, D. L. Nelson, F.-Y. Leung, Q. Li, D. J. Diner, and J. A. Logan. 2008. Wildfire smoke injection heights—two perspectives from space. Geophysical Research Letters 35:L04809.

Kashparov, V. A., S. M. Lundin, S. I. Zvarich, V. I. Yoschenko, S. E. Levtchuk, Y. V. Khomutinin, I. N. Maloshtan, and V. P. Protsak. 2003. Territory contamination with the radionuclides representing the fuel component of Chernobyl fallout. Science of the Total Environment 317:105–119.

Kempeneers, P., F. Sedano, L. Seebach, P. Strobl, and J. San-Miguel-Ayanz. 2011. Data fusion of different spatial resolution remote sensing images applied to forest type mapping. IEEE Transactions on Geoscience and Remote Sensing 49:4977–4986.

Krawchuk, M. A., and M. A. Moritz. 2011. Constraints on global fire activity vary across a resource gradient. Ecology 92:121–132.

Kristiansen, N. I., A. Stohl, and G. Wotawa. 2012. Atmospheric removal times of the aerosol-bound radionuclides ^{137}Cs and ^{131}I measured after the Fukushima Dai-ichi nuclear accident—a constraint for air quality and climate models. Atmospheric Chemistry and Physics 12:10759–10769.

Lavoue, D., C. Liousse, H. Cachier, B. J. Stocks, and J. G. Goldammer. 2000. Modeling of carbonaceous particles emitted by boreal and temperate wildfires at northern latitudes. Journal of Geophysical Research 105:26871–26890.

Leung, F.-Y., J. A. Logan, R. Park, E. Hyer, E. Kasischke, D. Streets, and L. Yurganov. 2007. Impacts of enhanced biomass burning in the boreal forests in 1998 on tropospheric chemistry and the sensitivity of model results to the injection height of emissions. Journal of Geophysical Research 112:D10313.

Linkov, I., S. Yoshida, and M. Steiner. 2000. Fungi contaminated by radionuclides: critical review of approaches to modeling. *In* Proceedings of the 10th International Congress of the International Radiation Protection Association (IRPA-10), Hiroshima, Japan, 14–19 May 2000, P-4b-255. http://www.irpa.net/irpa10/cdrom/00967.pdf

Long, N. Q., Y. Truong, P. D. Hien, N. T. Binh, L. N. Sieu, T. V. Giap, and N. T. Phan. 2012. Atmospheric radionuclides from the Fukushima Dai-ichi nuclear reactor accident observed in Vietnam. Journal of Environmental Radioactivity 111:53–58.

Lujanieneo, G., A. Plukis, E. Kimtys, V. Remeikis, D. Jankünaiteo, and B. I. Ogorodnikov. 2002. Study of ^{137}Cs, ^{90}Sr, ^{239,240}Pu, ^{238}Pu and ^{241}Am behavior in the Chernobyl soil. Journal of Radioanalytical and Nuclear Chemistry 251:59–68.

MacGarigal, K., and B. Marks. 1994. Fragstats: spatial pattern analysis program for quantifying landscape structure. Version 3. Oregon State University, Corvallis, Oregon, USA.

Masson, O., et al. 2011. Tracking of airborne radionuclides from the damaged Fukushima Dai-Ichi nuclear reactors by European networks. Environmental Science and Technology 45:7670–7677.

McDowell, N., et al. 2008. Mechanisms of plant survival and mortality during drought: why do some plants survive while others succumb to drought? New Phytologist 178:719–739.

McMullin, S., G. K. Giovanetti, M. P. Green, R. Henning, R. Holmes, K. Vorren, and J. F. Wilkerson. 2012. Measurement of airborne fission products in Chapel Hill, NC, USA from the Fukushima Dai-ichi reactor accident. Journal of Environmental Radioactivity 112:165–170.

Møller, A. P., A. Bonisoli-Alquati, G. Rudolfsen, and T. A. Mousseau. 2012. Elevated mortality among birds in Chernobyl as judged from skewed age and sex ratios. PLoS ONE 7:e35223.

Møller, A. P., K. A. Hobson, T. A. Mousseau, and A. M. Peklo. 2006. Chernobyl as a population sink for Barn Swallows: tracking dispersal using stable isotope profiles. Ecological Applications 16:1696–1705.

Møller, A. P., and T. A. Mousseau. 2013. Assessing effects of radiation on abundance of mammals and predator–prey interactions in Chernobyl using tracks in the snow. Ecological Indicators 26:112–116.

Mouillot, F., M. G. Schultz, C. Yue, P. Cadule, K. Tansey, P. Ciais, and E. Chuvieco. 2014. Ten years of global burned area products from spaceborne remote sensing—a review: analysis of user needs and recommendations for future developments. International Journal of Applied Earth Observation and Geoinformation 26:64–79.

Mousseau, T. A., G. Milinevsky, J. Kenney-Hunt, and A. P. Møller. 2014. Highly reduced mass loss rates and increased litter layer in radioactively contaminated areas. Oecologia 175:429–437.

Mousseau, T. A., S. M. Welch, I. Chizhevsky, O. Bondarenko, G. Milinevsky, D. J. Tedeschi, A. Bonisoli-Alquati, and A. P. Møller. 2013. Tree rings reveal extent of exposure to ionizing radiation in Scots pine *Pinus sylvestris*. Trees 27:1443–1453.

National Report of Ukraine (NRU). 2011. Reports Proceedings, conclusions and recommendations. *In* Twenty-five years after Chernobyl accident. Safety for the future. Proceedings of the International Conference, April 20–22, KIM Kyiv, Ukraine. Government of Ukraine, Kiev, Ukraine.

Nuclear Energy Agency (NEA). 2002. Chernobyl: assessment of radiological and health impacts. 2002 Update of Chernobyl: ten years on. Organisation for Economic Co-Operation and Development, Paris, France. https://www.oecd-nea.org/rp/reports/2003/nea3508-chernobyl.pdf

Paatero, J., J. Vira, M. Siitari-Kauppi, J. Hatakka, K. Holmén, and Y. Viisanen. 2012. Airborne fission products in the high Arctic after the Fukushima nuclear accident. Journal of Environmental Radioactivity 114:41–47.

Paliouris, G., H. W. Taylor, R. W. Wein, J. Svoboda, and B. Mierzynski. 1995. Fire as an agent in redistributing fallout ^{137}Cs in the Canadian boreal forest. Science of the Total Environment 160/161:153–166.

Paugam, R., M. Wooster, G. Papadakis, and M. Schultz. 2010. Estimation of the injection height of biomass burning emission. *In* Proceedings of the ESA-iLEAPS-EGU joint conference, Frascati, Italy.

Piga, D. 2010. Residence time of Cs-137 in the atmosphere. Dissertation. Université du Sud Toulon, Var, France.

Poiarkov, V. A. 1995. Post-Chernobyl radiomonitoring of the forest ecosystem. Journal of Radioanalytical and Nuclear Chemistry Archives 194:259–267.

Potter, C. S., J. T. Randerson, C. B. Field, P. A. Matson, P. M. Vitousek, H. A. Mooney, and S. A. Klooster. 1993. Terrestrial ecosystem production: a process model based on global satellite and surface data. Global Biogeochemical Cycles 7:811–841.

Raffa, K. F., B. H. Aukema, B. J. Bentz, A. L. Carroll, J. A. Hicke, M. G. Turner, and W. F. Romme. 2008. Cross-scale drivers of natural disturbances prone to anthropogenic amplification: the dynamics of bark beetle eruptions. BioScience 58:501–517.

R Development Core Team. 2014. R 3.1.0. R Project for Statistical Computing, Vienna, Austria. www.r-project.org

Raich, J. W., A. E. Russell, K. Kitayama, W. J. Parton, and P. M. Vitousek. 2006. Temperature influences carbon accumulation in moist tropical forests. Ecology 87:76–87.

Rio, C., F. Hourdin, and A. Chédin. 2010. Numerical simulation of tropospheric injection of biomass burning products by pyro-thermal plumes. Atmospheric Chemistry and Physics 10:3463–3478.

Scafetta, N., and B. J. West. 2006. Phenomenological solar contribution to the 1900–2000 global surface warming. Geophysical Research Letters 33:L05708.

Schlesinger, W. H. 1997. Biogeochemistry: an analysis of global change. Second edition. Academic Press, San Diego, California, USA.

Shand, C. A., M. V. Cheshire, S. Smith, M. Vidal, and G. Rauret. 1994. Distribution of radiocaesium in organic soils. Journal of Environmental Radioactivity 23:285–302.

Sitch, S., et al. 2003. Evaluation of ecosystem dynamics, plant geography and terrestrial carbon cycling in the LPJ Dynamic Global Vegetation Model. Global Change Biology 9:161–185.

Smith, J. E., and L. S. Heath. 2002. A model of forest floor carbon mass for United States forest types. Research Paper NE-722. USDA Forest Service, Newtown Square, Pennsylvania, USA.

Sofiev, M., T. Ermakova, and R. Vankevich. 2012. Evaluation of the smoke injection height from wild-land fires using remote sensing data. Atmospheric Chemistry and Physics 12:1995–2006.

Sofiev, M., R. Vankevich, T. Ermakova, and J. Hakkarainen. 2013. Global mapping of maximum emission heights and resulting vertical profiles of wildfire emissions. Atmospheric Chemistry and Physics 13:7039–7052.

Szopa, S., et al. 2012. Aerosol and Ozone changes as forcing for climate evolution between 1850 and 2100. Climate Dynamics 40:2223–2250.

Tanaka, K., Y. Takahashi, A. Sakaguchi, M. Umeo, S. Hayakawa, H. Tanida, T. Saito, and Y. Kanai. 2012. Vertical profiles of Iodine-131 and Cesium-137 in soils in Fukushima Prefecture related to the Fukushima Daiichi nuclear power station accident. Geochemistry Journal 46:73–76.

Thonicke, K., A. Spessa, I. C. Prentice, S. P. Harrison, L. Dong, and C. Carmona-Moreno. 2010. The influence of vegetation, fire spread and fire behaviour on biomass burning and trace gas emissions: results from a process-based model. Biogeosciences 7:1991–2011.

Thonicke, K., S. Venevsky, S. Sitch, and W. Cramer. 2001. The role of fire disturbance for global vegetation dynamics: coupling fire into a dynamic global vegetation model. Global Ecology and Biogeography 10:661–678.

United Nations Development Programme (UNDP) and United Nations Children's Fund (UNICEF). 2002. The human consequences of the Chernobyl nuclear accident. UNDP and UNICEF, New York, New York, USA. http://www.unicef.org/newsline/chernobylreport.pdf

Urbanski, S. P., W. M. Hao, and B. Nordgren. 2011. The wildland fire emission inventory: western United States emission estimates and an evaluation of uncertainty. Atmospheric Chemistry and Physics 11:12973–13000.

Urbanski, S. P., J. M. Salmon, B. L. Nordgren, and W. M. Hao. 2009. A MODIS direct broadcast algorithm for mapping wildfire burned area in the western United States. Remote Sensing of Environment 113:2511–2526.

Val Martin, M., C. L. Heald, B. Ford, A. J. Prenni, and C. Wiedinmyer. 2013. A decadal satellite analysis of the origins and impacts of smoke in Colorado. Atmospheric Chemistry and Physics 13:7429–7439.

Val Martin, M., J. A. Logan, R. Kahn, F.-Y. Leung, D. Nelson, and D. Diner. 2010. Smoke injection heights from fires in North America: Analysis of five years of satellite observations. Atmospheric Chemistry and Physics 10:1491–1510.

van der Werf, G. R., J. T. Randerson, and G. J. Collatz. 2003. Carbon emissions from fires in the tropical and subtropical ecosystems. Global Change Biology 9:547–562.

van der Werf, G. R., J. T. Randerson, L. Giglio, G. J. Collatz, M. Mu, P. S. Kasibhatla, D. C. Morton, R. S. DeFries, Y. Jin, and van T. T. Leeuwen. 2010. Global fire emissions and the contribution of deforestation, savanna, forest, agricultural, and peat fires (1997–2009). Atmospheric Chemistry and Physics 10:11707–11735.

van Mantgem, P. J., and N. L. Stephenson. 2007. Apparent climatically-induced increase of mortality rates in a temperate forest. Ecological Letters 10:909–916.

van Mantgem, P. J., N. L. Stephenson, L. S. Mutch, V. G. Johnson, A. M. Esperanza, and D. J. Parsons. 2003. Growth rate predicts mortality of *Abies concolor* in both burned and unburned stands. Canadian Journal of Forest Research 33:1029–1038.

Vicente-Serrano, S. M., S. Beguería, J. Lorenzo-Lacruz, J. J. Camarero, J. I. López-Moreno, C. Azorin-Molina, J. Revuelto, E. Morán-Tejeda, and A. Sanchez-Lorenzo. 2012. Performance of drought indices for ecological, agricultural, and hydrological applications. Earth Interactions 16:1–27.

Wang, R., et al. 2013. High-resolution mapping of combustion processes and implications for CO_2 emissions. Atmospheric Chemistry and Physics 13:5189–5203.

Westerling, A. L., H. G. Hidalgo, D. R. Cayan, and T. W. Swetnam. 2006. Warming and earlier spring increase western U.S. forest wildfire activity. Science 313:940–943.

Williams, A. P., et al. 2013. Temperature as a potent driver of regional forest drought stress and tree mortality. Nature Climate Change 3:292–297.

Woodhead, D. S. 1973. Levels of radioactivity in the marine environment and the dose commitment to the marine organisms. IAEA, Vienna, Austria.

Xiao, J., and Q. Zhuang. 2007. Drought effects on large fire activity in Canadian and Alaskan forests. Environmental Research Letters 2:044003.

Yablokov, A. V., V. B. Nesterenko, and A. V. Nesterenko. 2009. Chernobyl: consequences of the catastrophe for people and nature. New York Academy of Sciences, New York, New York, USA.

Yoschenko, V. I., V. A. Kashparov, M. D. Melnychuk, S. E. Levchuk, Y. O. Bondar, M. Lazarev, M. I. Yoschenko, E. B. Farfán, and G. T. Jannik. 2011. Chronic irradiation of Scots pine trees (*Pinus sylvestris*) in the Chernobyl Exclusion Zone: dosimetry and radiobiological effects. Health Physics 101:393–408.

Yoschenko, V. I., et al. 2006. Resuspension and redistribution of radionuclides during grassland and forest fires in the Chernobyl exclusion zone: part I. Fire experiments. Journal of Environmental Radioactivity 86:143–163.

Zibtsev, S. V., C. D. Oliver, J. G. Goldammer, A. M. Hohl, and O. A. Borsuk. 2011. Wildfires management and risk assessment in the Chernobyl Nuclear Power Plant Exclusion Zone. *In*: Twenty-five years after Chernobyl accident. Proceedings of the 5th International Wildland Fire Conference, Sun City, South Africa, 9–13 May 2011.

Supplemental Material

Ecological Archives

The Appendix is available online: http://dx.doi.org/10.1890/14-1227.1.sm

Data Availability

Data associated with this paper have been deposited in Dryad: http://dx.doi.org/10.5061/dryad.33mn2